Studies of molecular features and novel prognostic biomarkers of cutaneous melanoma

Iva Johansson

Department of Oncology
Institute of Clinical Sciences
Sahlgrenska Academy, University of Gothenburg

UNIVERSITY OF GOTHENBURG

Gothenburg 2022

Cover photo: Primary cutaneous malignant melanoma that metastasized to the brain. Copyright Iva Johansson 2022.

Studies of molecular features and novel prognostic biomarkers of primary cutaneous melanoma

iva.johansson@gu.se

ISBN 978-91-8069-021-8 (PRINT)
ISBN 978-91-8069-022-5 (PDF)
Printed in Borås, Sweden 2022
Printed by Stema Specialtryck AB

“Liksom de första femton dagarna för en planta, måste de första femton orden i en berättelse innehålla allt som berättelsen behöver för att överleva. Bara jag får ihop dessa femton ord, kommer resten av orden att rinna till, har jag tänkt. Bara jag lyckas ta mig över femtonordströskeln är det klart.”

-Bodil Malmsten *Priset på vatten i Finistère*

To my Czech and Swedish family and friends

Mé české a švédské rodině a přátelům

Studies of molecular features and novel prognostic biomarkers of cutaneous melanoma

Iva Johansson

Department of Oncology, Institute of Clinical Sciences
Sahlgrenska Academy, University of Gothenburg
Gothenburg, Sweden

ABSTRACT

Cutaneous malignant melanoma is a highly heterogeneous disease. Immunotherapy has revolutionized the treatment of stage IV disease and is now successfully administered as adjuvant treatment in stage III. Important prognostic features in the early phase of the disease are found within the primary tumor and sentinel lymph node, but plenty is still to be investigated. Sentinel lymph node biopsy (SLNB) status is one of the independent prognostic factors guiding treatment decisions, but not without controversy. Approximately 80% of the SLNB are negative, contrasting to a wide range of prognosis in node-negative patients. In paper I, we explored the molecular features of melanoma arising in chronic sun-damage skin showing that this type of melanoma is a distinct molecular entity with a different progression compared to the more common melanoma in intermittently sun-exposed skin. In papers II and III, we evaluated a novel non-invasive prognostic test to be utilized in primary cutaneous melanoma. The CP-GEP test was able to safely identify the patients where the sentinel lymph node biopsy is unnecessary. The same CP-GEP test was able to stratify the patients with high and low risk of disease progression, but the algorithm still needs to be optimized for this purpose in a clinical setting. In paper IV, we showed that digital quantification of crucial inflammatory cells in the primary tumor microenvironment using immunohistochemistry has the potential to further identify primary melanoma at high risk of brain metastasis.

Keywords: Primary cutaneous melanoma, chronic sun-damage skin, gene expression profiling, immunohistochemistry, tertiary lymphoid structures, B cells, CD8+ T cells, brain metastasis

ISBN978-91-8069-021-8(PRINT)
ISBN978-91-8069-022-5 (PDF)

SAMMANFATTNING PÅ SVENSKA

Malignt melanom med ursprung i huden ökar stadigt och är en av de mest aggressiva tumörsjukdomarna med ca 4500 nya fall och 500 dödsfall per år i Sverige. UV strålningen utgör den viktigaste orsaksfaktorn. Tumörerna med denna benämning varierar stort beträffande sitt makroskopiska och mikroskopiska utseende, molekylära karakteristika, samt inte minst tendensen att sprida sig till andra dela av kroppen, svara på given behandling och slutligen leda till döden. Immunterapi med användning av s k immuncheckpointhämmare har revolutionerat behandlingen av spritt melanom som tidigare varit mestadels obotligt. Immunterapi kan hos 40-50 % av patienter med spridd sjukdom leda till en långvarig respons och ges nu även som tilläggsbehandling till patienter med melanom med hög risk för spridning. Det är viktigt att identifiera patienter som kommer att ha nytta av behandlingen då denna kan ha allvarliga och långvariga biverkningar. Riskfaktorerna för en mer allvarlig sjukdom med risk för vidare spridning står bland annat att finna i modertumören som bortoperats från huden. Tumörens tjocklek mätt vid mikroskopisk undersökning avgör merparten av prognosen. Patienterna med tumörtjocklek överstigande 1 mm erbjuds även en undersökning av portvaktkörteln som bortorereras. Påvisning av dottertumör i portvaktkörteln indikerar en sämre prognos. Denna undersökning innebär ett kirurgiskt ingrepp med risk för biverknigar. Dessutom sprider sig många melanom till övriga kroppen trots att portvaktkörteln varit negativ. I studie I genomfördes molekylära studier av melanom som upkommer i kroniskt solskadad hud, den näst vanligaste melanomtypen i Sverige. Resultaten visar att denna typ av melanom drivs av andra mutationer och progredierar annorlunda än superficiellt spridande melanom, den vanligaste melanomtypen. I studierna II och III har vi i ett stort kliniskt material från Sahlgrenska sjukhuset utvärderat ett nytt genetiskt test (CP-GEP) som kan identifiera melanompatienter som inte behöver genomgå en portvaktkörtelundersökning. En tredjedel av patienterna med melanomtjocklek 1-2 mm skulle med hög grad av säkerhet kunna avstå från portvaktkörtelundersökningen. Samma test har visat sig kunna särskilja patienter med hög, respective låg risk för sjukdomsåterfall men testmetodiken behöver finjusteras innan det kan vara aktuellt med användning i klinisk rutinsjukvård. I studie IV har vi genomfört en digital analys av immunceller i anslutning till hudmelanom i immunfärgade histologiska snitt. I vårt material var mängden CD8+ och CD20+ lymfocyter signifikant lägre i melanom som senare metastaserat till hjärnan jämfört med tumörer som inte spridits vidare trots långtidsuppföljning. Metoden behöver utvärderas i ett större patientmaterial avseende dess potential som prognostisk biomarkör.

LIST OF PAPERS

This thesis is based on the following studies, referred to in the text by their Roman numerals.

I. Sanna A, Harbst K, **Johansson I**, Christensen G, Lauss M, Mitra S, Rosengren F, Hakkinen J, Vallon-Christersson J, Olsson H, Ingvar A, Isaksson K, Ingvar C, Nielsen K, Jonsson G.
Tumor genetic heterogeneity analysis of chronic sun-damaged melanoma.
Pigment Cell Melanoma Res 2020;33(3): 480-489.

II. **Johansson I**, Tempel D, Dwarkasing JT, Rentroia-Pacheco B, Mattsson J, Ny L, Olofsson Bagge R.
Validation of a clinicopathological and gene expression profile model to identify patients with cutaneous melanoma where sentinel lymph node biopsy is unnecessary.
Eur J Surg Oncol. 2022 Feb;48(2):320-325.

III. Mulder EEAP*, **Johansson I***, Grünhagen DJ, Tempel D, Rentroia-Pacheco B, Dwarkasing JT, Verver D, Mooyaart AL, van der Veldt AAM, Wakkee M, Nijsten TEC, Verhoef C, Mattsson J, Ny L, Hollestein LM*, Olofsson Bagge R*. Using a Clinicopathologic and Gene Expression (CP-GEP) Model to Identify Stage I-II Melanoma Patients at Risk of Disease Relapse.
Cancers (Basel). 2022 Jun 9;14(12):2854.
*these authors have contributed equally

IV. **Johansson I**, Arheden A, Jespersen H, Carstam L, Matsson J, Akyürek L, Olofsson BaggeR, Ny L.
Presence of CD8+ and CD20+ lymphocytes and tertiary lymphoid structures in the invasion zone of primary cutaneous melanoma and the association to brain metastasis.
Manuscript

RELATED PAPERS NOT INCLUDED IN THESIS

i. Mirzaei N, Katsarelias D, Zaar P, Jalnefjord O, **Johansson I**, Leonhardt H, Wärnberg F, Olofsson Bagge R. Sentinel lymph node localization and staging with a low-dose of superparamagnetic iron oxide (SPIO) enhanced MRI and magnetometer in patients with cutaneous melanoma of the extremity - The MAGMEN feasibility study. *Eur J Surg Oncol*. 2022;48(2):326-332.

ii. Theodosiou G, **Johansson I**, Hamnerius N, Svensson Å. Naevoid Malignant Melanoma: A Diagnosis of a Naevus That You Later Regret. *Acta Derm Venereol*. 2017;97(6):745-746.

iii. Crescitelli R, Lässer C, Jang SC, Cvjetkovic A, Malmhall C, Karimi N, Hoog JL, **Johansson I**, Fuchs J, Thorsell A, Gho YS, Olofsson Bagge R, Lotvall J. Subpopulations of extracellular vesicles from human metastatic melanoma tissue identified by quantitative proteomics after optimized isolation. *J Extracell Vesicles*. 2020;9(1):1722433.

iv. Cabrita R, Lauss M, Sanna A, Donia M, Skaarup Larsen M, Mitra S, **Johansson I**, Phung B, Harbst K, Vallon-Christersson J, van Schoiack A, Lovgren K, Warren S, Jirstrom K, Olsson H, Pietras K, Ingvar C, Isaksson K, Schadendorf D, Schmidt H, Bastholt L, Carneiro A, Wargo JA, Svane IM, Jonsson G. Tertiary lymphoid structures improve immunotherapy and survival in melanoma [published correction appears in Nature. 2020 Apr;580(7801): E1]. *Nature*. 2020;577(7791):561-565.

v. Sjödahl G, Abrahamsson J, Holmsten K, Bernardo C, Chebil G, Eriksson P, **Johansson I**, Kollberg P, Lindh C, Lövgren K, Marzouka N, Olsson H, Höglund M, Ullén M, Liedberg F. Different Responses to Neoadjuvant Chemotherapy in Urothelial Carcinoma Molecular Subtypes. *Eur Urol*. 2022;81(5):523-532.

vi. Christensen GB, Nagaoka T, Kiyohara Y, **Johansson I**, Ingvar C, Nakamura A, Sota T, Nielsen K. Clinical performance of a novel hyperspectral imaging device for cutaneous melanoma and pigmented skin lesions in Caucasian skin. *Skin Res Technol*. 2021;27(5):803-809.

vii. Benton S, Zhao J, Zhang B, Bahrami A, Barnhill RL, Busam K, Cerroni L, Cook MG, de la Fouchardiere A, Elder DE, **Johansson I**, Landman G, Lazar A, LeBoit P, Lowe L, Massi D, Duncan LM, Messina J, Mihic-Probst D, Mihm MC, Jr., Piepkorn MW, Schmidt B, Scolyer RA, Shea CR, Tetzlaff MT, Tron VA, Xu X, Yeh I, Yun SJ, Zembowicz A, Gerami P. Impact of Next-generation Sequencing

on Interobserver Agreement and Diagnosis of Spitzoid Neoplasms. *Am J Surg Pathol*. 2021;45(12):1597-1605.

viii. **Johansson I**, Levin M, Akyürek LM, Olofsson Bagge R, Ny L. PD-1 inhibitor therapy of basal cell carcinoma with pulmonary metastasis. *J Eur Acad Dermatol Venereol*. 2022;36 Suppl 1:70-73.

ix. Sanna A, Phung B, Mitra S, Lauss M, Choi J, Zhang T, Njauw CJ, Cordero E, Harbst K, Rosengren F, Cabrita R, **Johansson I**, Isaksson K, Ingvar C, Carneiro A, Brown K, Tsao H, Andersson M, Pietras K, Jönsson G. DNA promoter hypermethylation of melanocyte lineage genes determines melanoma phenotype [published online ahead of print, 2022 Aug 30]. *JCI Insight*. 2022; e156577.

x. Moncrieff MD, Lo SN, Scolyer RA, Heaton MJ, Nobes JP, Snelling AP, Carr MJ, Nessim C, Wade R, Peach AH, Kisyova R, Mason J, Wilson ED, Nolan G, Pritchard Jones R, **Johansson I**, Olofsson Bagge R, Wright LJ, Patel NG, Sondak VK, Thompson JF, Zager JS. Clinical Outcomes and Risk Stratification of Early-Stage Melanoma Micrometastases from an International Multicenter Study: Implications for the Management of American Joint Committee on Cancer IIIA Disease [published online ahead of print, 2022 Jul 18]. *J Clin Oncol*. 2022; JCO2102488.

CONTENT

ABBREVIATIONS

CSD	Chronic sun-damage
ICI	Immune checkpoint inhibitor
CMM	Cutaneous malignant melanoma
SSM	Superficial spreading melanoma
AJCC	American Joint Committee on Cancer
WHO	World Health Organization
NMM	Nodular malignant melanoma
LMM	Lentigo maligna melanoma
SLNB	Sentinel lymph node biopsy
SLN	Sentinel lymph node
CLND	Completion lymphadenectomy
WLE	Wide local excision
EMT	Epithelial mesenchymal transition
MITF	Melanocyte inducing trascription factor
PAX genes	Paired box genes
SOX genes	SRY-related HMG box genes
FOX genes	Forkhead box genes
TYR gene	Tyrosinase gene
PMEL	Premelanosome protein
MLANA gene	Melanoma antigen recognized by T cells gene

DNA	Deoxyribonucleic acid
MSH	Melanocyte-stimulating hormone
POMC	Proopiomelanocortin
ACTH	Adrenocorticotropic hormone
HMB-45	Human melanoma black (monoclonal antibody)
ITGB	Integrin beta
MCAM	Melanoma cell adhesion molecule
ICAM	Intercellular adhesion molecule
DCT	Dopachrome tautomerase
UVR	Ultra-violet radiation
CDKN2A	Cyklin dependent kinase inhibitor 2A
BAP1	BRCA1 Associated Protein 1
TERT	Telomerase reverse transcriptase
BRAF	B-Raf proto-oncogene
NRAS	N-ras proto-oncogene
PIK3CA	Phosphatidylinositol-4,5-Bisphosphate 3-Kinase Catalytic Subunit Alpha
ROS	ROS proto-oncogene
NTRK	Neurotrophic receptor tyrosine kinase
ALK	ALK receptor tyrosine kinase
MET	MET proto-oncogene
RET	RET proto-oncogene
CCND	Cyclin D

GNAQ	G protein subunit alpha Q
GNA11	G protein subunit alpha 11
CYSLTR	Cysteinyl Leukotriene receptor
PLCB4	Phospholipase C Beta 4
SF3B1	Splicing Factor 3b Subunit 1
EIF1AX	Eukaryotic Translation Initiation Factor 1A X-Linked
MSS	Melanoma specific survival
TMB	Tumor mutational burden
RNA	Ribonucleic acid
PD-L1	Programmed death-ligand 1
PD-1	Programmed cell death protein 1
CTLA-4	Cytotoxic T-lymphocyte antigen 4
TILs	Tumor infiltrating lymphocytes
LDH	Lactate dehydrogenase
IL	Interleukin
CXCL	Chemokine (C-X-C motif) ligand
TCR	T cell receptor
ctDNA	Circulating tumor DNA
BD	Breslow depth (interchangeble with Breslow thickness)
H&E	Hematoxylin and Eosin
MIA	Melanoma Institute Australia
MSKCC	Memorial Sloan Kettering Cancer Center

FISH	Fluorescent in situ hybridization
GEP	Gene expression profiling
cDNA	Complementary DNA
NGS	New generation sequencing
IHC	Immunohistochemistry
CD	Cluster of differentiation
Ig	Immunoglobulin
TLS	Tertiary lymphoid structures
RTK	Receptor tyrosine kinase
NF1	Neurofibromin 1
MAPK	Mitogen-Activated Protein Kinase
BBB	Blood brain barrier
(CAR) T cells	Chimeric antigen receptor T cells
ACT	Adoptive cell therapy
BM	Brain metastasis (or MBM for melanoma brain metastasis)

INTRODUCTION

Malignant melanoma is a feared disease constituting one of the most malignant tumors in humans. It possesses the highest mortality rate among the common skin cancer types, despite the commonly small size of the primary tumor. Sometimes, it can be difficult to diagnose both macroscopically and microscopically(1). Its most common form originates from the pigment-synthesizing cells in the skin, the melanocytes. Queensland in Australia is leading with an annual incidence of 72/100 000 (2, 3) but also in Sweden, the incidence and prevalence are among the highest in the world(4). The Swedish annual incidence is 43/100 000 in men and 36/100 000 in women, with a 5 % constant annual increase for several decades. In Sweden, every year, approximately 4500 new invasive melanomas are diagnosed, and 500 patients die of the disease(5). Besides representing a devastating disease for the individual patient, also the resources used in the management of melanoma confer high healthcare costs ranging from a general practitioner and specialist care, including biopsies, surgical excisions, skin grafts, radiology, sentinel lymph node biopsy (SLNB) and completion lymphadenectomy, surgical removal of metastases, immunotherapy, targeted systemic and local oncologic therapies, and follow-up care. Immune checkpoint inhibitors (ICIs) have greatly improved melanoma-specific survival, with approximately half of the patients being long-term responders(6). Melanoma is highly curable by surgical excision at an early stage, and the histopathologic evaluation of the excised primary melanoma, in select cases, along with the SLNB(7), deliver the most important but far from perfect prognostic factors for the management of the early-stage disease. Selection of patients for various kinds of costly and even life-threatening therapies benefits from specific and sensitive prognostic and predictive factors to tailor the individual treatment, which makes the purpose for further research in this field.

1.1 MELANOCYTES

Melanocytes are pigment-synthesizing cells located in the stratified squamous epithelium in the epidermis, and in hair follicles, uvea, the inner ear, meninges, the brain, and the heart(8-11).

1.1.1 EMBRYOGENESIS AND MELANOCYTIC LINEAGE GENES

Understanding the fundamental principles of embryogenesis, such as the epithelial-mesenchymal transition (EMT) and the opposite process of the mesenchymal-epithelial transition, is crucial for understanding important

mechanisms in the evolution and progression of malignant tumors. Like other forms of cancer, melanoma may adopt the embryonal mechanisms of EMT and acquire the potential of leaving the original tissue site, moving through the underlying mesenchyme, settling down in a new environment, and setting up colonies through adaptation to the local metabolic conditions(12). Melanocytic precursors, the melanoblasts, develop during embryogenesis within the neural crest. *Neural crest* is a bilateral linear embryogenic structure that forms and detaches from the neural tube through epithelial-mesenchymal transition at embryonal week 4(13). The pluripotent progenitor cells (SOX10+) of melanocytes, glia, and neurons within the neural crest undergo EMT and become highly migratory and proliferative. The subsequent activation of MITF separates the cells into two lineages, the melanoblasts (MITF+) and glial neuronal precursors (MITF-)(14, 15). MITF is the main transcription factor in the melanocytic lineage, governing the development, survival, and function of melanocytes(16). Transcription factors PAX3 and SOX10 activate MITF transcription(17). Mutations in either MITF, PAX3, or SOX10 result in Waardenburg syndrome with various changes in facial appearance, pigmentation, and congenital hearing loss(18). The initial activation of MITF is dependent on low levels of two additional transcription factors, FOXD3 and SOX2 (upregulated in future glial cells and neurons and downregulated during the development of melanoblasts)(19). Melanoblasts migrate along the dorsolateral and ventral pathways through the mesenchyme to reach their foremost final destination, the basal epidermis and the bulb of hair follicles. Melanoblasts acquire KIT expression and differentiate to pigment-producing melanocytes (TYR+) within the hair bulbs and the epidermis. A subset of melanoblasts ($MITF^{low}$, KIT^{low}) form a reservoir of melanocyte stem cells in the hair bulge to be activated during the hair cycle, wound healing, and regeneration after vitiligo(20). Normal melanocytes share many features with melanoma. Understanding the normal mechanisms involved in the development, migration, differentiation, proliferation, regeneration, interaction with surrounding cells, and apoptosis of the normal melanocytes is necessary for understanding important skin diseases such as melanoma, albinism, and vitiligo(21). TYR gene encodes tyrosinase, the enzyme that catalyzes the initial steps in the conversion of tyrosine to melanin. Mutations in this gene result in oculocutaneous albinism. PMEL gene encodes GP-100, a glycoprotein involved in melanosome maturation, expressed in normal melanocytes and a high proportion of melanoma(22). Targeting gp-100 by Tebentafusp has been recently implemented in the treatment of uveal melanoma(23). MLANA gene encodes a surface protein MART-1, highly specific for melanocytes. The expression of both MART-1 and GP-100 is transcriptionally regulated by MITF(24). The KIT gene encodes a receptor tyrosine kinase which, when activated, catalyzes phosphorylation of a number of intracellular proteins involved in differentiation, proliferation, migration,

and apoptosis of several cell types, including melanocytes. Activating genomic alterations involving KIT have been found in melanoma in chronic sun-damaged skin as well as the acral and mucosal subtypes. Imatinib, nilotinib, and sunitinib are targeted drugs with efficacy in KIT overactive tumors(25).

1.1.2 NORMAL MELANOCYTES IN THE EPIDERMIS

Melanocytes are located within the basal epidermis, and their primary function is to protect the DNA from the mutagenic effect of UV radiation. Melanin pigment is synthesized during melanogenesis, and mature melanosomes are transported via long dendritic processes into the cytoplasm of the neighboring keratinocytes. *The epidermal melanin unit* consists of 36 keratinocytes that receive melanin from one melanocyte(26).

Melanin is synthesized by melanocytes in response to alpha-melanocyte-stimulating hormone (α-MSH), which increases mainly in response to DNA damage by UV in the keratinocytes. Even other physiologic and pathophysiologic mechanisms involve hypersecretion secretion of alpha-melanocyte-stimulating hormone (α-MSH), resulting in hyperpigmentation in pregnancy, Addison´s disease, and acanthosis nigricans in Cushing´s disease. The common denominator in these processes is proopiomelanocortin (POMC), which is synthesized in keratinocytes, melanocytes and anterior pituitary. POMC is post-translationally cleaved into peptides, such as α-MSH, ACTH, and β-endorphin(27-29). Synthetic analogs of α-MSH, such as afamelanotide (Melanotan,) are used to enhance tanning for both aesthetic and medical reasons(30, 31). Animal *melanin* is a polymeric protein synthesized from the amino acid tyrosine in melanosomes. As a phylogenetically ubiquitous biologic material, melanin has a very high refractive index and a broad absorption spectrum for effective protection from ultraviolet, visible, and infrared rays. In humans, three different melanins are produced from a common precursor, eumelanin, pheomelanin, and neuromelanin(32). Eumelanin and pheomelanin are always found in a combination of both in various proportions, resulting in different hair and skin color(33). Melanosomes are specialized organelles derived from endosomes and their function is to synthesize and store melanin. Melanosomes are found at four different stages, where stage II contains a glycoprotein gp100 (recognized by HMB-45 antibody). A visible, electron-dense protein is produced in later stages III and IV. Stage IV melanosomes are subsequently transported to keratinocytes through a hitherto unclear process(34). *Lentigo solaris* is an example of a CSD^{high} skin lesion where disruption in normal melanin synthesis, transfer, or turnover has occurred(35, 36).

Melanocytes reside in the basal epidermis embedded between surrounding basal keratinocytes in typical ratio of 1:10. The cells are oval with dendritic processes. The nuclei are smaller with a more dense chromatin structure compared to the surrounding keratinocytes. In formalin-fixed paraffin-embedded sections, there is an artifactual halo around the nucleus. Normal melanocytes are attached to surrounding keratinocytes and basal membrane matrix via E-cadherin and Integrin beta 7. Loss of expression of adhesion molecules is associated with the early steps of melanoma development and metastasis. Additionally, some adhesion proteins ITGB3, MCAM, and ICAM1 are expressed in melanoma, enhancing proliferation, survival, and metastasis(37).

Normal melanocytes are characterized by mutual contact inhibition in contrast to neoplastic processes such as melanocytic nevi and melanoma, where melanocytes coexist in apposition to each other. Mechanisms behind normal contact inhibition are largely unknown. Chronic-sun damage skin shows an increased density with some degree of confluence of epidermal melanocytes even in the absence of a melanocytic neoplasm(38).

Differentiated mature cutaneous melanocytes constitute a stablecell population characterized by an extremely low rate of proliferation. Mechanisms involved in normal melanocytic proliferation arrest are unknown. The number of melanocytes decreases with age by 10-20% for every decade after the age of 30(39). Normal melanocytes depend on trophic signaling through paracrine factors and cell adhesion mediated by *keratinocytes* and dermal *fibroblasts*(40, 41), such as during physiological hyperplasia in melanocytes overlying maturing scar-tissue or fibrous histiocytoma(42), as well as hyperplasia of melanocytes within benign and malignant keratinocytic tumors.

Normal melanocytes are poorly distinguishable in routine histologic stains. However, they may be clearly visualized using antibodies specific for proteins such as melanosomal matrix proteins (MART-1), SOX10, tyrosinase (TYR), tyrosinase-related proteins 1 and 2 (TYRP1, TYRP2/DCT), microphthalmia transcription factor (MITF), and S-100(43).

1.2 MELANOMA AND OTHER MELANOCYTIC TUMORS

Malignant melanoma is a malignant tumor of melanocytes. Melanoma represents the malignant end of the spectrum of melanocytic tumors with the potential to metastasize and kill the patient. *Melanocytic tumors* are neoplastic lesions fueled by mutations and epigenetic changes, shaped by the tumor microenvironment. The tumor progression in melanocytic tumors is associated with changes in cytomorphology, accumulation of mutations and structural abnormalities of the DNA, changes in gene expression and in vitro characteristics(44). Melanoma shows one of the highest numbers of mutations among solid tumors, with a median of 10 mutations per Mb. Interestingly, even non-lesional skin harbors 2-6 mutations per Mb(45, 46). This fact has at least two immediate implications i.e., it makes melanoma a highly immunogenic cancer, as well as it provides the background for the broad spectrum of morphological appearances and biological behavior. Melanocytic tumors are categorized as *benign*, *intermediate,* and *malignant*. Histologic examination is the gold standard for the diagnosis of melanocytic tumors. Both early superficial and late tumorigenic lesions may sometimes pose severe diagnostic difficulties and remain *ambiguous* despite broad immunohistochemical panels and use of molecular tests. In recent years, several categories of intermediate lesions were defined through the integration of morphology, clinical features and the molecular background. These lesions include deep penetrating melanocytoma, BAP-1 inactivated tumor, pigmented epithelioid melanocytoma, and BRAF-mutated spitzoid tumor.

1.2.1 RISK FACTORS OF MELANOMA

UV radiation is the most significant risk factor for the development of the majority of melanomas, accounting for approximately 90 % of the tumors(47). UVC is completely filtered by the atmosphere. Radiation with longer wave lengths, UVB and UVA reach the surface of the Earth. The highest levels are present at high altitudes, especially when reflected by snow and in places close to the equator or underlying defects in the ozone layer. UVB is highly mutagenic and penetrates the epidermis and superficial dermis, causing DNA damage within the cells in the tissue. UVA penetrates deeper into the dermis and is responsible for skin aging. Apart from outdoor exposure, indoor tanning in solariums and sun lamps constitute another important source of UV damage(48). Around 10% of the patients with melanoma exhibit a family history of the disease, even though *true hereditary melanoma* is even more

rare. The most common types of melanoma-predisposing germline gene variants are found within CDKN2A, accounting for 40% of familial melanoma cases. Additionally, CDKN2A mutations confer a high risk of pancreatic cancer, head and neck cancer, and lung cancer(49). Mutations in CDK4(50), BAP1(51, 52), POT1(53), and TERT promoter(54), found in sporadic melanoma, are very rare in a germline setting. Fair complexion, freckles, blue eyes, multiple melanocytic nevi, immunosuppression, and DNA repair defects predispose to melanoma development more complexly. Male gender and truncal location are linked to higher mortality(55).

1.3 WHO CLASSIFICATION OF MELANOCYTIC TUMORS 4TH EDITION

After a gap of nearly ten years, the fourth edition of the WHO classification of melanocytic tumors was introduced in 2018. The classification took off from the recent advances in molecular studies of the progression of melanocytic tumors from benign precursors to melanoma. Nine pathways to melanoma were outlined according to the clinical, histological, molecular,and, epidemiological characteristics of the melanocytic neoplastic processes. Seven pathways cover the primary cutaneous melanoma, and the resting two are uveal melanoma and mucosal melanoma. In several pathways, intermediate lesions were defined and diagnostically categorized between the clearly benign and clearly malignant tumors. Due to UV being the main mutagenic factor in melanoma, the majority of human melanomas originate in sun-exposed fair skin, and these are described within classes I-III. Chronic sun damage is graded according to the UV-related changes in elastin structure within the dermis(56) (**Figure 1**). The other subtypes of melanoma in class IV-IX are not etiologically related to UV exposure(57). Assigning a tumor to the correct pathway is a critical and fundamental component of the diagnostical process, as demonstrated by tumors with BAP1 loss. This phenomenon occurs both in melanocytomas within pathway I and tumors on the malignant side of the spectrum within pathways VIII and IX(58). *P16* is a commonly used immunohistochemical marker in melanocytic pathology, and the *loss of p16*

needs to be carefully evaluated within the context of the pathway where it had occurred(59, 60).

Figure 1. Chronic sun damage skin with solar elastosis grade III, as proposed by Landi et al. (H&E, original magnification x100).

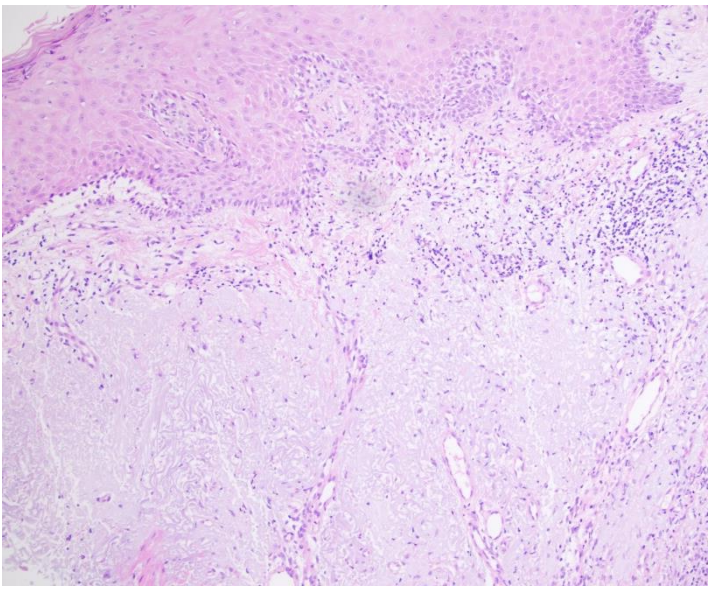

1.3.1 CSD^{LOW} MELANOMA

CSD^{low} melanoma is synonymous with superficial spreading melanoma (SSM), with a characteristic radial growth phase (RGP) even though a portion exhibits a nodular architecture. This type of melanoma is the most common and the best- understood type, accounting for more than 70% of melanoma. It arises in non-glabrous fair skin in association with intermittent sun exposure. It is associated with low-grade of chronic sun damage, pagetoid scatter, epithelioid cytomorphology, frequent mitoses, nested growth pattern, and frequent BRAF V600E mutations (**Figure 2**). The tumors are often well-circumscribed and pigmented. The common precursors are acquired melanocytic nevi. Dysplastic nevi, BAP-1 inactivated tumor, deep penetrating melanocytoma and pigmented epithelioid melanocytoma represent intermediate lesions within this class.

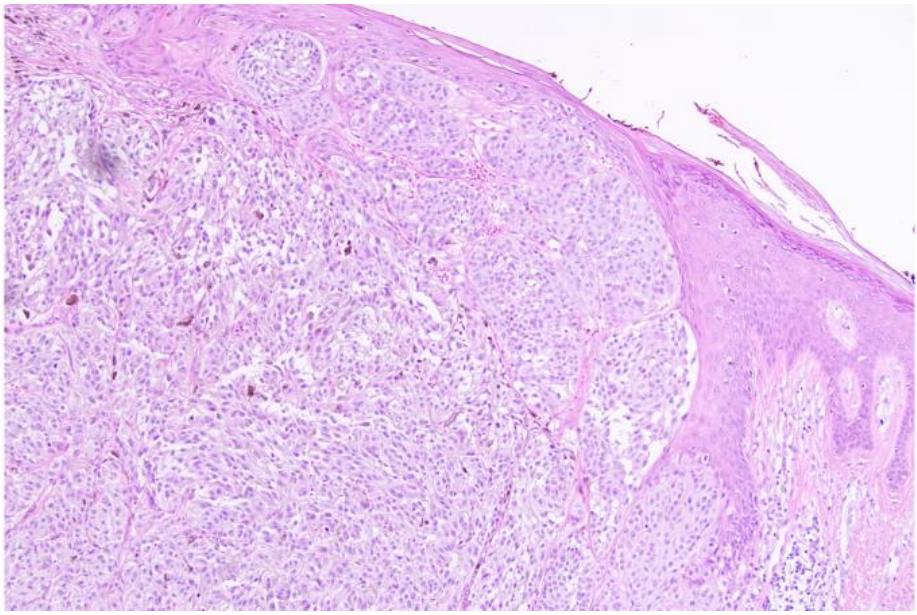

Figure 2. Part of superficial spreading melanoma, CSDlow melanoma. In dermis are large nests of atypical pleomorphic elongated cells. The epidermis is acanthotic with focal thinning. (H&E, original magnification x100).

1.3.2 CSD^{HIGH} MELANOMA

CSD^{high} melanoma is synonymous with lentigo maligna melanoma. It is the second most common melanoma in Western countries, corresponding to approximately 10 % of melanoma in Sweden. It afflicts older persons than SSM melanoma. The precursor lesion is poorly defined. Lentigo maligna, which represents the melanoma in situ form within this pathway, is a slowly

growing pigmented macule, most commonly on the face of the elderly. Histologically, the intraepidermal tumor cells grow in a lentiginous pattern, small nests, and usually moderate to severe cytologic atypia (**Figure 3**). They grow within a highly specific microenvironment with an atrophic flat epidermis and a high grade of solar elastosis in the underlying dermis. The characteristic genomic features are BRAF non V600E, NF1, NRAS, and KIT mutations in the context of a very high mutation burden and predominant UV signature(61, 62).

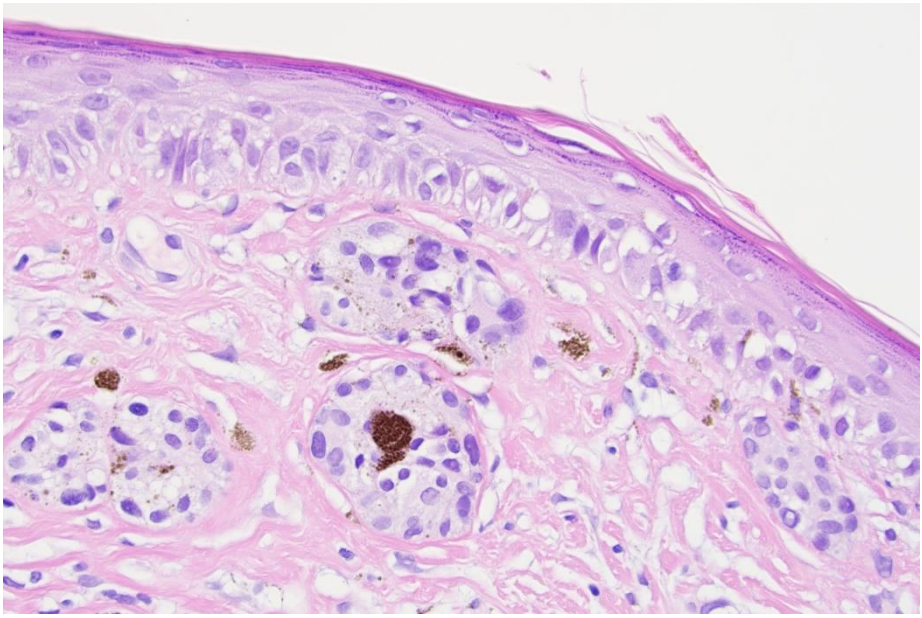

Figure 3. Lentigo maligna melanoma (CSDhigh melanoma), Breslow thickness 0.4 mm, pT1a. Prominent lentiginous in situ component, a small area of dermal invasion with minor nests and individual cells. No mitoses. Coarse melanin granules within melanophages. (H&E, original magnification x400).

1.3.3 DESMOPLASTIC MELANOMA

Desmoplastic melanoma is a rare form of melanoma, accounting for 4 % of cutaneous melanomas, most commonly slowly growing and arising in CSD^{high} skin. It may pose severe diagnostic difficulties due to the lack of pigmentation and scar-like appearance both clinically and histologically. Pure (>90% of the dermal component) desmoplastic melanoma has a good prognosis despite the commonly pronounced Breslow thickness. This entity is defined by the dermal component composed of spindled wavy melanocytes within a desmoplastic scar-like stroma(63), immunohistochemical reactivity for S100 and SOX10

but negative for MART-1 and HMB-45. The in situ component is often inconspicuous or lentigo maligna. Desmoplastic melanoma has an extremely high mutation burden, harboring inactivating NF1 mutations, NFKBIE promoter mutations, and various activating mutations in MAPK and PIK3C pathways (MAP2K1, MAP3K1, BRAF, EGFR, MET, RAC1, PIK3CA, NRAS)(64).

1.3.4 MALIGNANT SPITZ TUMOR (SPITZ MELANOMA)

Spitz melanoma is very rare, and the diagnosis requires both specific cytomorphology and architecture together with driver mutations in HRAS or kinase fusions typical for the Spitz trajectory (involving ALK, MET, ROS1, RET, NTRK1, NTRK3, BRAF and MAP3K8) commonly along with TERT promoter mutations and homozygous loss of P16, P14 and P15. Cytologically the tumor cells are large spindle and/or epithelioid with abundant amphophilic hyaline cytoplasm, large irregular nuclei and prominent nucleoli. The term "spitzoid melanoma" refers to bona fide SSM melanoma with spitzoid cytomorphology and architecture(60).

1.3.5 ACRAL MELANOMA

Acral melanoma arises in the glabrous skin of palms and soles and the nail apparatus and is unrelated to UV exposure. It occurs in all ethnic groups and is the most common type of melanoma in non-Caucasian populations. It is characterized by a few point mutations in BRAF, NRAS, KIT(65), and kinase fusions of ALK and RET(66). The tumor mutation burden is characteristically low compared to the UV-related melanoma subtypes and the tumors harbor structural rearrangements and amplifications of KIT, TERT, CCND1, CDK4, MITF and TERT(67). Repetitive trauma has been suggested as a predisposing factor for the development of this kind of melanoma(68).

1.3.6 MUCOSAL MELANOMA

Mucosal melanoma is a rare form of melanoma, non-UV related, occurring at equal frequency in all ethnic groups. The tumors arise on mucosal surfaces of the oral and nasal cavity, genital and anal sites, and conjunctiva. It comprises 1% of all melanomas and carries a poor prognosis. The precursor lesion has not been clearly defined. In likelihood with acral melanoma, the genetic background encompasses a low mutation burden and various copy number changes and structural variants, together with NRAS and KIT mutations(69).

1.3.7 MELANOMA ARISING IN CONGENITAL NEVUS

This type of melanoma is uncommon and arises within giant congenital nevi, typically during childhood. The majority of these melanomas harbor activating NRAS mutations(70). TERT promoter methylation has been described as a mechanism contributing to malignant transformation within this category(71).

1.3.8 MELANOMA ARISING IN BLUE NEVUS

This subtype of melanoma is extremely rare and arises within the uncommon precursor lesion, the cellular blue nevus. It is characterized by an increased number of chromosomal aberrations (>3), mutations in protein G signaling pathway (GNAQ, GNA11, CYSLTR2, PLCB4), monosomy 3, gains of 8q and copy number changes in SF3B1, EIF1AX.

1.3.9 UVEAL MELANOMA

Uveal melanoma is a rare type of melanoma arising in the eye´s choroidea, ciliary body, and iris. In Sweden, approximately 80 persons per year are affected by the disease. Metastases are most often localized to the liver and carry a poor prognosis. The genetic background overlaps extensively with those of melanoma arising in blue nevi. Typically, the driving mutations are within the protein G pathway (GNAQ, GNA11, CYSLTR2, PLCB4), as well as BAP1, SF3B1, and EIF1AX(72).

1.4 AJCC VERSION 8

Melanoma staging describes the stages of tumor progression. It is associated with disease prognosis (**Fig.4**). In clinical stage I, the tumor is confined to the superficial skin, and the Breslow thickness underscores 1 mm. Stage II encompasses tumors still localized to the skin but with a thickness over 1 mm in the presence of ulceration. Stage III is for tumors with a regional spread, including satellites and in transit metastases, or with metastasis in regional lymph nodes. Stage IV means tumors with distant metastasis. 5-years melanoma-specific survival ranges from 99% in stage IA to 22% in stage IV(73). The Eighth edition of the AJCC melanoma staging system was

T	Breslow and T substage	N	M	Clinical stage
Tis		N0	M	0
T1	≤1.0 mm			
	T1a[1]	N0	M0	IA
	T1b[2]	N0	M0	IB
T2	>1.0-2.0 mm			
	T2a	N0	M0	IB
	T2b	N0	M0	IIA
T3	>2.0-4.0 mm			
	T3a	N0	M0	IIA
	T3b	N0	M0	IIB
T4	>4mm			
	T4a	N0	M0	IIB
	T4b	N0	M0	IIC
Any T, Tis		≥N1	M0	III
Any T		Any N	M1	IV

Node (N)	Description	M	Clinical stage
Nx	Regional nodes cannot be assesed	M0	-
N0	No melanoma in regional nodes	M0	IA-IIB
N1	Melanoma in one node or in-transit/satellite/microsatellites	M0	III
N1a	Microscopic metastasis in one node	M0	IIIA-IIIC
N1b	Macroscopic metastasis in one node	M0	IIIB-IIIC
N1c	In-transit or satellite or microsatellite metastases	M0	IIIC
N2	Melanoma in two or three nodes	M0	III
N2a	Microscopic metastasis in two or three nodes	M0	IIIA-IIIC
N2b	Macroscopic metastasis in two or three nodes	M0	IIIB-IIIC
N2c	In-transit or satellite lesions without nodal metastasis	M0	IIIC
N3	Melanoma in four or more nodes, or matted nodes, or in-transit or satellite lesions with nodal metastasis	M0	IIID

Metastasis(M)	Description	Clinical stage
Mx	Metastasis cannot be assessed	-
M0	No distant metastasis	IA-IIID
M1a	Metastasis to skin, subcutis, muscle or distant nodes	IV
M1b	Metastasis to lung	IV
M1c	Metastasis to non-CNS visceral sites	IV
M1d	Metastasis to CNS	IV

Table 1. Clinical stages of melanoma are based on various combinations of T, N and M stages. Adapted from Gershenwald et al.2018

implemented in 2018(74), aiming to improve staging, risk-stratification, prognostication and selection of patients with melanoma for treatment modalities and clinical trials. The important changes compared to the previous version were changes in the determinants of primary tumor status within the T1 category, changes in the determinants of the N regional lymph node status, new groups within stage III due to a wide range of melanoma-specific survival rates (stage IIIa 93% five-year MSS and stage IIID 32%) and a new designation of brain metastasis M1d within the M category.

1.5 BIOMARKERS IN CUTANEOUS MELANOMA

Biomarkers are objective, quantifiable characteristics of biological processes and constitute the base of precision medicine. Biomarkers can be classified as *tumor-intrinsic* (Breslow thickness, ulceration, mitotic density, mutational status, TMB, RNA expression profile, PD-L1 expression), *microenvironmental* (TILs) and *systemic* (LDH, S100B, IL-6, IL-8, CXCL-5, microbiota, inflammatory cell counts, TCR repertoire, ctDNA)(75).

Predictive biomarkers predict clinical outcomes associated with treatment.

Prognostic biomarkers inform the patient´s overall outcome, regardless of treatment.

1.5.1 HISTOPATHOLOGIC PROGNOSTIC MARKERS IN SURGICAL EXCISIONS OF PRIMARY CUTANEOUS MELANOMA

Breslow thickness

Breslow thickness is the most important prognostic factor in primary melanoma and a cornerstone of the eighth version of the AJCC staging of melanoma. The method is a tribute to the late US pathologist Alexander Breslow. He presented his research in 1970(76), and the method has kept its leading position within melanoma diagnostics. It is an independent prognostic factor for melanoma survival, also able to predict the risk of lymph node

metastasis. The five years tumor-specific survival ranges from 95-100% in patients with BD < 1mm to 50% in patients with BD > 4 mm. Regarding T1 melanoma, there is a critical threshold for the survival risk at BD 0.7 to 0.8 mm, as already suggested by the original author more than 50 years ago. BD measurement requires a histologic examination of the primary tumor. With only a few caveats, it is a simple, robust, and readily reproducible tumor parameter measured from the granular layer of the epidermis or from the bottom of tumor ulceration to the deepest tumor cell in the underlying tissue. Other closely related methods, such as Breslow density, have been proposed, but these are not in clinical use yet(77).

Ulceration

Ulceration of the primary tumor represents another histologic staging parameter in the current AJCC staging system. Ulceration implies a worse prognosis and is histologically defined as a full-thickness loss of the covering epidermal epithelium overlying the primary melanoma with melanoma cells facing the surface. Ulcerated tumors are designated with the suffix “b” within each T stage. The only exceptions are T1b tumors, where even non-ulcerated tumors with Breslow thickness 0,75-1,04 mm (rounded up to 0,8 -1,0 mm) are categorized as “b”. The interobserver agreement and reproducibility are excellent regarding this parameter(78).

Mitotic rate

It is well established that a high mitotic rate in primary melanoma is an independent prognostic factor associated with lower melanoma-specific survival(79). In the previous (seventh) version of the AJCC staging, T1b melanomas were defined as those with Breslow thickness ≤ 1mm and at least one mitosis/mm^2(80). Despite the evidence of the value of assessing this parameter, mitotic rate was discharged from the eighth version of AJCC due to results from the multivariate analysis showing that utilizing Breslow thickness dichotomized at 0,8 mm outperforms mitotic rate as a dichotomous variable for prediction of melanoma-specific survival(81). Mitotic rate counting on H&E sections is labor-intensive and rather poorly reproducible(82). It should be performed within a 1-mm^2 “hot spot”. Perhaps the advent of routine digital pathology may initiate a renaissance of this parameter(83).

Sentinel lymph node status

Sentinel lymph node biopsy was introduced in 1992 by Morton and Cochrane(84, 85). The method has been continuously refined, applied to a wide range of malignancies, and also reevaluated in the management of melanoma. At present, sentinel lymph node biopsy is an important staging tool implemented in most national guidelines worldwide. The method requires identification of the sentinel lymph node by lymphoscintigraphy with Tc^{99m} or superparamagnetic iron oxide(86, 87). Upon surgical excision of the node with the highest signal, a histopathological examination utilizing various standard protocols with serial sectioning and immunohistochemistry is performed(88). Approximately 80% of the SLNBs render negative results. The indication for SLNB is the diagnosis of primary melanoma with Breslow thickness over 1 mm. When melanoma ≤1 mm is the subject for SLNB, the positivity frequency is lower, around 5. Breslow thickness, mitotic activity, or presence of ulceration do not safely predict SLNB positivity in thin melanomas. Younger age was appointed as a significant predictor of SLNB metastasis(89, 90). The utility of SLNB is an important staging instrument even for thick melanomas where SLNB status was the only predictor of melanoma-specific survival(91). Currently, patients with clinical stage IIIA are not eligible for adjuvant systemic therapy. However, a large multi-center study by Moncrief et al. showed that SN metastases ≥0.3 mm entails a higher risk of melanoma progression, and these patients might benefit from adjuvant systemic therapy(92).

1.5.2 PROGNOSTIC AND PREDICTIVE INSTRUMENTS

Several prognostic instruments available online are based on data from large patient registries. The Swedish prognostic instrument is based on data from 7500 patients that underwent SLNB for melanoma and calculates melanoma-specific survival at 1, 5, and 10 years after the primary melanoma excision. The input variables in this tool are SLNB status (if available), gender, age, tumor site, Breslow depth, presence of ulceration, and Clark level. The favorable prognostic factors are female gender, younger age, little Breslow depth, no ulceration, low Clark level and negative SLNB(93). Another online

tool is the Melanoma nomogram from the Memorial Sloan Kettering Cancer Center for the prediction of SLNB status. The input variables are Breslow depth, age at diagnosis, Clark level, tumor site, and presence of ulceration. The nomogram generates the percentage risk of having a positive SLNB(94, 95). Melanoma Institute Australia (MIA) has presented five prognostic and prediction tools, such as the Sentinel Node Metastasis risk tool, which requires the input of Breslow thickness, melanoma subtype, ulceration, lymphovascular invasion, number of mitoses/mm^2, and the patient´s age. The output is the percentage risk of having a positive SLNB(96-98). Another MIA instrument, the Thin Melanoma Recurrence Risk, is based on data from the MIA patient database and the Dutch national melanoma registry (PALGA) and requires the input of the tumor site, Breslow thickness, melanoma subtype, presence of mitoses, ulceration, the patient´s age, gender, and SLNB status to generate the percentage risk score for a local, regional and distant recurrence respectively(99, 100).

1.5.3 DNA SEQUENCING AND GENE EXPRESSION PROFILING IN MELANOCYTIC LESIONS

Molecular tests used in melanocytic tumors have been designed for different purposes and use various techniques.

1. *Ancillary tests* for the diagnosis of ambiguous melanocytic lesions where histopathology may not clearly distinguish between benign and malignant lesion: Comparative genomic hybridization (CGH) and single nucleotide polymorphism array (SNP) are based on the fact that most melanomas harbor multiple chromosomal abnormalities in contract to nevi or low-risk lesions which usually show <3(59). FISH is useful for the same purpose, especially in situations where the amount of available tumor DNA is limited. The presence of TERT promoter mutations analyzed by Sanger sequencing indicates a high-risk lesion or melanoma(101). Gene expression profiling (GEP) utilizing reverse transcription of RNA to cDNA and real-time PCR is the basis of several commercially available tests(102).

2. *Prognostic tests* for melanoma encompass algorithm-based computation of risk of disease recurrence or sentinel lymph node positivity using gene expression profiling, sometimes in combination with various clinical parameters: Decision Dx melanoma(103), MelaGenix(104), CP-GEP test(105, 106).

3. *Predictive tests* for response to targeted therapy include the detection of actionable mutations crucial for indicating BRAF, MEK, and KIT inhibitors (107, 108). Sequencing of parts of the melanoma genome is routinely performed in stage III and IV melanoma. A minority of detected mutations have clear therapeutic implications. The rest of the output from large NGS panels has a less well-defined relevance.

1.5.4 TUMOR MUTATIONAL BURDEN (TMB)

Total mutation burden represents the total number of somatic mutations per million bases (Mb) of a tumor genome and is a measure of all non-synonymous coding mutations in the tumor exome. The mutation rate varies widely between various tumor types. Pediatric and hematologic malignancies harbor a low number of mutations (< 1 mutation/Mb), and melanoma is located on the opposite side of the spectrum (>10 mutations/Mb).

Highly mutated tumors such as melanoma produce numerous neoantigens, some of which activating T cells. This provides a rationale for high TMB as a biomarker for response to PD-1/PD-L1 inhibitors. High TMB is associated with improved response to immune checkpoint inhibitors. The degree of TMB may be assessed by whole-genome sequencing, whole-exome sequencing, and targeted panel sequencing. The highly mutagenic effect of UV exposure is the cause of the high TMB in subsets of melanoma. Low sensitivity in the determination of TMB may be caused by low tumor cell purity(46, 109).

1.5.5 PD-L1 TESTING

The immunologic synapse within the tumor microenvironment is highly complex. The interaction between PD-L1and PD-1 molecules is one of the major modulators of the immune system aiming to avoid autoimmunity in a normal host. PD-L1 is important in the regulation of immune surveillance of the tumor microenvironment dynamics and kinetics. Cancer cells may upregulate PD-L1, leading to immune suppressive signals and evasion of immune surveillance. Previous studies have characterized the PD-L1 expression using immunohistochemistry, believing that an expression of PD-L1 protein would be strongly associated with response rates to immune checkpoint inhibitors (nivolumab, pembrolizumab, atezolizumab). Unfortunately, PD-L1 is neither a highly specific nor sensitive biomarker due

to tumor intrinsic PD-L1 heterogeneity and its plasticity during tumorigenesis in an individual patient(110, 111). Many patients with the expression of PD-L1 do not respond to immunotherapy, and contrariwise some patients without PD-L1 expression do benefit. Hence, this marker does not function well as a stratifier of patients who will benefit from ICI treatment(112). There are multiple caveats in PD-L1 testing, such as a significant variability (7-15%) in the scoring of PD-L1 staining between the different IHC assays. The retrospective studies evaluating the potential interchangeability are rather small and few. Further validation in prospective studies, including samples of patients with immune checkpoint inhibition, is still needed(113). Apart from the PD-1-PD-L1 system, additional immune checkpoints have been identified (**Figure 4**).

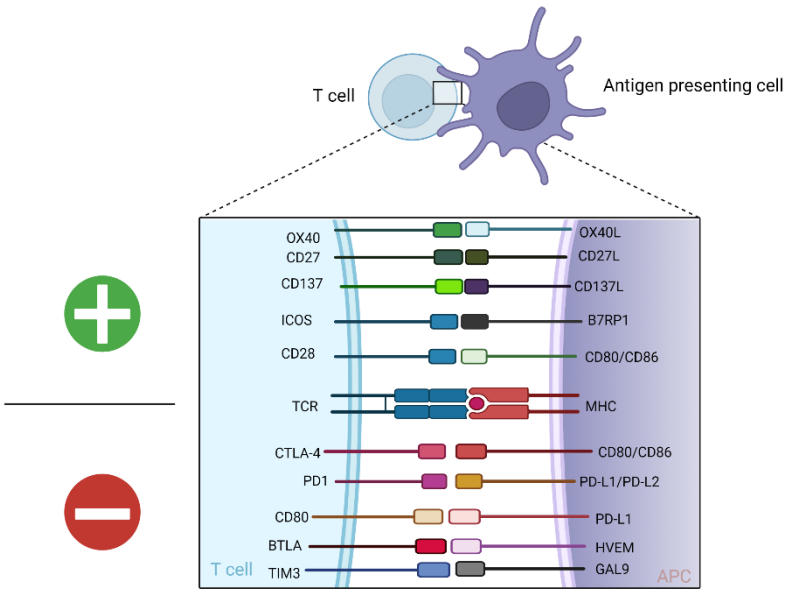

Figure 4. Co-stimulatory (+) and co-inhibitory (-) checkpoints involved in T cell activation. Adapted from Coana et al. Created with Biorender.com

1.5.6 IMMUNE RESPONSES IN MELANOMA

Immune surveillance is a vital physiologic mechanism protecting the body against the establishment of malignancy. Immune-compromised individuals are prone to develop cancer(114). Inflammation in association with melanoma

is an important constituent of the tumor microenvironment where the tumor and inflammation continuously shape each other. Tumor-infiltrating lymphocytes (TILs), dendritic cells, macrophages, neutrophils, and natural killer cells interact with the tumor cells and each other through intricate mechanisms (**Figure 6**). There are several approaches for evaluating of the inflammatory tumor microenvironment; histologically by simply reporting the presence or absence of the certain cell types, by quantifying of the cells, or by spatial analyses with various degrees of the complexity of the phenotypic characterization of the inflammatory cells and their interactions. The presence of tertiary lymphoid structures in primary and metastatic melanoma was associated with a better prognosis and response to immunotherapy(115). Another approach involves predictive gene signatures concerning antigen presentation, T-cell genes, immune checkpoints, chemokine and cytokine profiles of the inflammatory environment. Single-cell RNA sequencing reveals the diversity of the inflammatory cell phenotypes and cell states. Markers of both inflammatory cell activation, dysfunction, and exhaustion are studied. Preclinical evidence has been emerging, but to date, no method safely identifies responders and non-responders to immunotherapy. Melanoma arising in chronic sun damage skin is commonly highly inflamed already in the in situ stage (**Figure 5**).

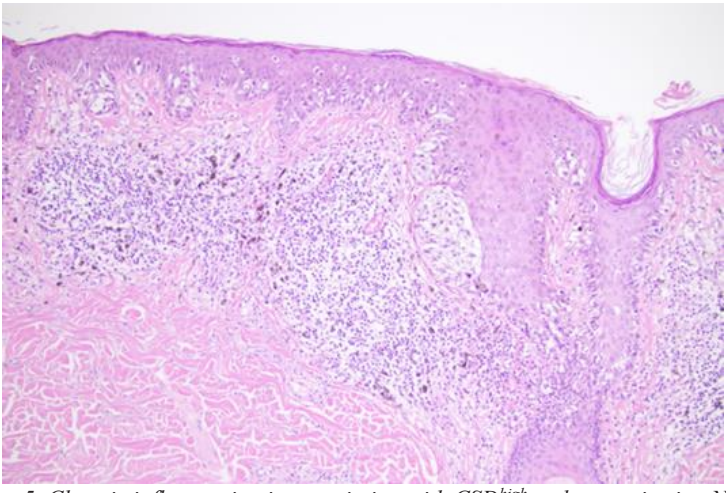

Figure 5. Chronic inflammation in association with CSD^{high} melanoma in situ. Note the dense lymphocytic infiltrate with melanophages and stromal reaction in papillary dermis. (H&E original magnification 200x).

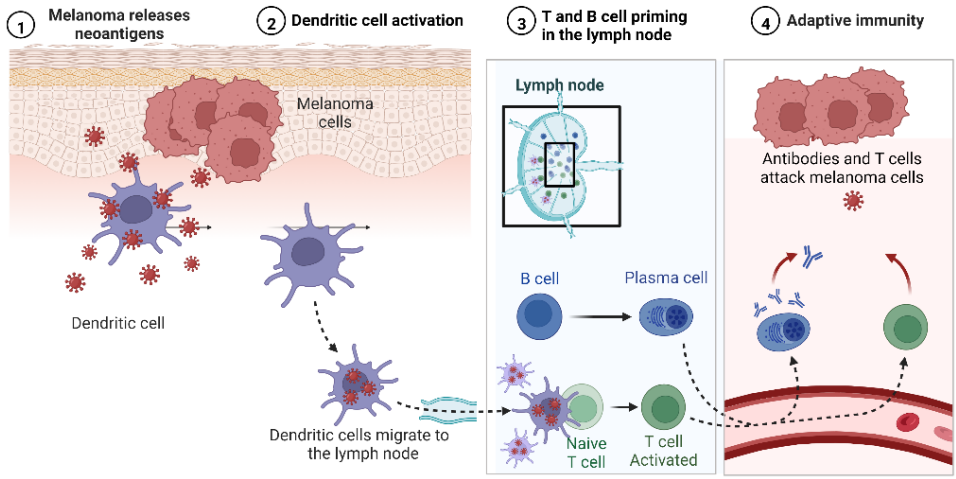

Figure 6. Activation of T and B cells in lymph nodes. Created with Biorender.com.

T cells

T lymphocytes are involved in continuous anti-tumor surveillance in the body, and upon activation, they migrate toward evolving neoplastic lesions (**Figure 6**). T-cell activation requires antigen presentation on MHC molecules interacting with the TCR and is fine-tuned through numerous co-stimulatory and co-inhibitory signals (**Figure 4**). Two major subtypes of T lymphocytes, CD4+ and CD8+, have different roles within anti-tumor immunity. CD4+ T helper lymphocytes recognize melanoma-neoantigens as peptides presented on MHC class II surface molecules of dendritic cells, macrophages, and B-lymphocytes, and become activated. Cytotoxic CD8+ T-lymphocytes recognize peptides presented on MHC class I molecules present on all cells with nucleus. When activated, CD8+ cell may kill the cells with a matching MHC I-bound peptide by secreting toxic molecules granzyme B and perforin (**Figure 7**). Tumor cells are continuously shaped by the inflammatory environment which exerts selection pressure on the tumor. There are multiple immune checkpoints on the surface of T cells modulating the immune responses (**Figure 4**).

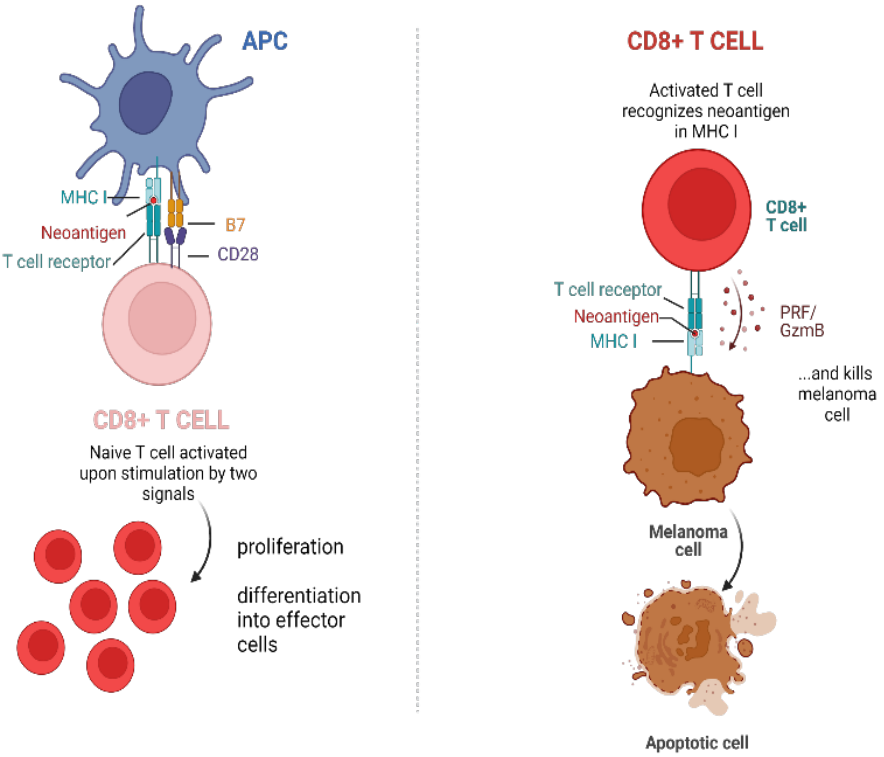

Figure 7. Activation of cytotoxic CD8+ T lymphocytes by neoantigen presented on dendritic cells. Effector mechanism in melanoma. Abbreviation: APC, antigen presenting cell; MHC, major histocompatibility complex; PRF, perforin; GzmB, granzyme B. Created with Biorender.com

molecules preventing a final cytotoxic attack. PD-L1 molecule that interacts with PD-1 on the surface of T lymphocytes, leads to deactivating of the T lymphocytes. This mechanism is crucial for physiologic prevention of autoimmunity but has been hijacked by multiple tumor types, including melanoma. Therapeutic immune checkpoint blockade unleashes the CD8+ cells that may then proceed with the cytotoxic activity. Regulatory T cells (T_{regs}) can with their CTLA-4 molecules capture CD80 ligands from the APC (mostly migratory dendritic cells). This process is called *transendocytosis* , thus preventing a T-cell stimulatory synapse between CD28 and CD80(116).

B cells

B cells are a crucial component of humoral immunity but elicit even cellular responses. The role of B cells in the tumor microenvironment is complex due to concurrent pro-tumor and anti-tumor activities and the activation of other cell types with the same spectrum of activities. They recognize antigens by membrane-bound surface immunoglobulins and when differentiated to plasma cells, also secrete immunoglobulins that attach to antigens in extracellular space (**Figure 8**). Naïve B cells harbor membrane bound IgM and IgD receptors. Upon binding of an antigen, the cell proliferates and differentiates to generate a few thousand of *plasma cells* with the same antigen specificity as the original naïve B cell. In contrast to T cells, antibodies are produced not only against peptides but also against polysaccharides, nucleic acids, lipids, and small molecules. Upon their differentiation process, B cells undergo heavy-chain *isotype (class) switch* and *affinity maturation* leading to the production of antibodies with an increasing affinity for the antigen. This process only, when involving protein-antigens is facilitated by CD4+ T helper cells with the same antigen specificity as the B cells. Most B cells (follicular B cells) reside in follicles in lymph nodes and take part in the intricate T-cell dependent high-affinity immunity involving protein antigens with the generation of plasma cells and memory B cells. The less common type, marginal B cells, reside within the spleen and govern more simple immunity against non-protein antigens (117). Extensive infiltration of B cells is associated with longer progression-free survival, overall survival, and improved outcomes of immunotherapy in several solid tumor types(115, 118, 119).

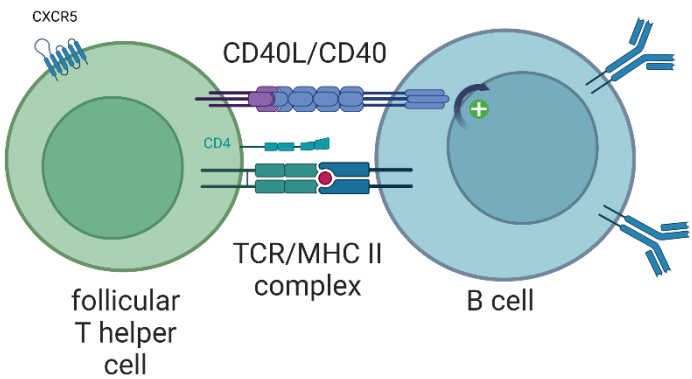

Figure 8. Activation of B cells by follicular T helper cells in lymphoid follicle. Created with Biorender.com.

Tertiary lymphoid structures

Tertiary lymphoid structures (TLS) are ectopic lymphoid organs with a function and architecture reminiscent of lymphoid follicles within lymph nodes. TLS develop at sites of chronic inflammation, both in tumors, autoimmune diseases, and infection. Hence, TLS do not develop in all patients(120). The initial immunological synapses between B and T helper cell generate low levels of low-affinity antibodies and short-lived plasma cells. To boost a robust immune response, some B cells move into germinal centers to interact with follicular T-helper cells and become activated (**Fig. 8**). B cells divide rapidly and form a light zone within the germinal center where the affinity maturation generates long-lived plasma and memory cells. TLS in cancer demonstrate various maturation states culminating in the formation of germinal centers. TLS have been appointed as a promising predictive and prognostic biomarker, but their value as such and the exact mechanisms of how the TLS stimulate T cells in the anti-cancer actions are still unclear(121).

1.6 THERAPY

1.6.1 SURGICAL THERAPY

Surgical removal of primary melanoma at the earliest possible stage has the highest impact on melanoma-specific survival of all possible treatments.

Lesions clinically suspicious for melanoma should be promptly removed by complete *excision* with a 2 mm clinical margin and sent for histological examination. When verified as invasive melanoma, further management is guided by the pathological stage of the excised lesion. For pT1a lesions, the next step is a wide local excision with a 1 cm margin. Patients with tumors pT2 and higher are offered further staging with sentinel lymph node biopsy. pT1b tumors are in most instances not an indication for SLN due to the low rate of positive findings in this category(122).

Until recently, completion lymph node dissection (CLND) was performed as the standard of care for patients with a positive sentinel lymph node. The rationale behind the automatic CLND was to increase the staging accuracy, better regional disease control, and improve the melanoma-specific survival. CLND is associated with postoperative morbidities, such as lymphedema,

pain, and tissue scarring, but there is still some staging value in uncovering the non-sentinel lymph node status. Metastasis in non- sentinel lymph nodes is an independent prognostic factor associated with higher recurrence rates and worse melanoma-specific survival(123). Two seminal clinical trials, DeCOG-SLT(124) and MSLT-II(125), did not demonstrate any difference in survival between patients treated with standard CLND and those monitored by nodal observation. CLND proved to be associated with a minor improvement of the local disease control and a small but significantly higher rate of disease-free survival at the three-year follow-up. DeCOG-SLT was criticized due to the small sample size (N=483) and short follow-up (35 months). The majority of patients in both studies had a low tumor burden (≤1 mm) in the SLNs, which may represent a substantial selection bias. Despite the criticism, the immediate CLND was abandoned as the standard of care for melanoma in most cases.

1.6.2 TARGETED THERAPY

Extensive data from the Cancer Genome Atlas (TCGA) on the genomic landscape of cutaneous melanoma enabled a genomic classification of melanoma into four subtypes (BRAF, RAS, NF1, and triple wild-type) that may guide clinical management with targeted therapies(126). *BRAF* mutations occur in approximately 50% of melanomas. Mutations in BRAF resulting in constitutive activation of the MAPK signaling pathway (**Fig.9**), BRAF V600E, V600K, V600M, and V600R are effectively targeted by BRAF inhibitors, often in combination with MEK inhibitors. BRAF non V600 mutations occur in less than 5% of melanoma and have a less clear clinical significance with variable responses to BRAF and MEK inhibitors(127). *NRAS* mutations occur in approximately 20-25% of melanoma and are associated with a poor response to MEK inhibitors. Q61R is the most common mutation. MEK inhibitors alone or combined with MAPK, PIK3, or CDK4 inhibition are under development(128). *KIT* is a receptor tyrosine kinase that, after ligand binding, activates the KIT protein with subsequent activation of multiple underlying signaling pathways. Mutations in KIT are rare, mostly occurring in acral, mucosal, and CSD^{high} melanoma. Receptor tyrosine kinase (RTK) inhibitors may be effective in up to 50% of KIT-mutated (exon 11) melanomas, but unfortunately, resistance to treatment occurs within one year. KIT-amplified melanomas do not respond to RTK inhibitors(129). For patients with *NF1* mutated melanoma, there are no established targeted therapies.

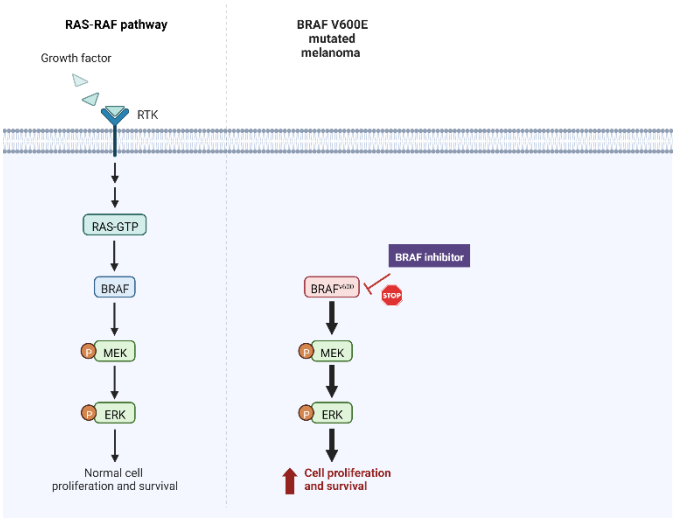

Figure 9. MAPK pathway with mutated BRAF protein resulting in activation of the pathway independent of signaling from the cell surface receptor. Created with Biorender.com

1.6.3 IMMUNOTHERAPY

Immune attack by the adaptive immune system is one of the most potent tools for eliminating cancer. Tumor cells can prevent cytotoxic cell actions of CD8+ T lymphocytes by synthesizing cell surface immune checkpoint molecules that inactivate the T cells trying to make an immunologic synapse with the tumor. Blocking of the immune checkpoint molecules by monoclonal antibodies leads to the reactivation of tumor-specific T cells and cytotoxic tumor cell death. Agents that target PD-1 (Programmed cell death protein 1) (**Figure 10**), PD-L1 (Programmed death ligand 1), and CTLA-4 (cytotoxic T-lymphocyte antigen 4) have revolutionized the therapy of a broad group of cancers, including melanoma. Approximately 40-50% of the patients with stage IV melanoma respond to immune checkpoint inhibitors (ICI), and the therapy may result in durable responses.

Apart from the development of antibodies targeting other immune checkpoint molecules (TIM-3, TIGIT, LAG3, VISTA), there are multiple other experimental and therapeutic principles to restore or enhance the host immune response to melanoma, such as chimeric antigen receptor (CAR)T cells, adoptive cell therapies (ACT), IL-2, bispecific antibodies, and cancer vaccines.

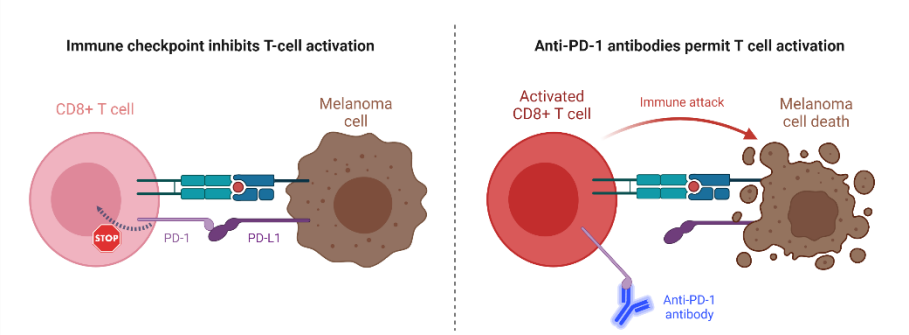

Figure 10. Principles of immune checkpoint blockade by monoclonal antibody directed toward PD-1 molecule. Created with Biorender.com.

1.7 BRAIN METASTASIS OF MELANOMA

Brain metastasis (BM) is a severe complication of cutaneous melanoma occurring in up to 50 % of patients with stage IV disease. The prevalence is up to 75% in autopsy series, indicating a high frequency of asymptomatic metastases(130, 131). Prognosis is inferior, with a median survival of 4-5 months after the BM diagnosis, even though the introduction of targeted therapy and ICI has improved the disease course and survival(132, 133). Treatment decisions are guided by the location, size, and number of the lesions in the brain(134). Stereotactic surgery, ICI and targeted therapy, sometimes in combination with radiotherapy, represent the current therapeutic strategies. The intact blood-brain barrier (BBB) prevents the uptake of molecules > 400 Da constituting an obstacle to drug delivery. Along with the disease progression, the BBB becomes compromised with an enhanced potential for drug delivery. Cerebrotropic melanoma acquires a specific phenotype with

expression of PLEKHA5, MMP2, and CD271 and down-regulation of MITF(135). Soluble factors secreted by astrocytes may play an essential role in phenotype switch, initiation, and maintenance of brain metastasis(136). In a study by Gardner et al., the risk factors predisposing to brain metastasis were scalp location, Breslow thickness> 4mm, nodular growth and ulceration. There was no difference between the outcomes of patients with asymptomatic and symptomatic BM(135, 137). Ideally, a specific biomarker predicting the risk of BM would be detected in the early stage of the disease, but the search for such has not been fruitful yet.

2 AIM

This thesis aims to contribute to the increasing knowledge of cellular clonality and malignant transformation of cutaneous melanoma in chronic sun-damage skin and evaluate new biomarkers for early-stage cutaneous melanoma.

SPECIFIC AIMS

Paper I

To explore the molecular features of the transition from in situ to invasive melanoma of high chronic sun-damage type and to investigate the intra-tumoral and early metastatic heterogeneity of this type of primary melanoma.

Paper II

To evaluate whether a novel test method for primary cutaneous melanoma using clinicopathologic and gene expression variables (CP-GEP; Merlin Assay) can identify patients who may safely forgo SLNB.

Paper III

To evaluate whether the same test method as in paper II (CP-GEP; Merlin Assay) can predict the risk of disease recurrence in patients with stage I-II melanoma.

Paper IV

To evaluate the potential of using subgroups of TILs as a histological biomarker for high-risk primary melanoma with immunohistochemistry and digital image analysis.

3 PATIENTS AND METHODS

3.1 PATIENT SAMPLES

3.1.1 PAPER I

Patient inclusion and the method for collection of samples were approved by the Regional Ethical Committee (Dnr 101/2013). Biopsies from primary cutaneous melanomas, both invasive and in situ, (n=72) in this study were part of BioMEL, a prospective study in Southern Sweden. Additionally, one patient without prior treatment to surgery for a large primary melanoma and surrounding in-transit metastases was included in the study. The patient had an ulcerated 25 mm diameter spindle cell melanoma arising in chronic sun-damaged skin on the shoulder, with a Breslow thickness of 16 mm, and multiple satellite and in-transit metastases.

3.1.2 PAPER II

The study was conducted in accordance with valid regulations upon approval of the Swedish Ethical Review Authority (Dnr 908-14). The patients were selected from a clinical database with patients undergoing SLNB after excision of primary cutaneous melanoma between 2006 and 2014 at the Sahlgrenska University Hospital, Gothenburg, Sweden (n = 489). The cohort included cutaneous melanoma from all body regions, except for the head and neck region. All primary tumors were reviewed and when necessary, re-staged according to valid AJCC and WHO criteria.
Of the 489 patients, a total of 425 patients met the inclusion criteria. The included patients had a single cutaneous melanoma, were >18 years, provided a written consent to research, had no history of Jacob Creutzfeldt disease, had primary tumor paraffin blocks containing a sufficient residual tumor tissue, and had no distant metastatic disease at primary melanoma diagnosis or within 90 days post diagnosis, no clinically positive nodes, full SN pathology report available and having a successful SLNB procedure.

3.1.3 PAPER III

The study was conducted as an international collaboration between two tertiary melanoma centers in Sweden and the Netherlands under approval by the

Swedish Ethical Review Authority (Dnr 908- 14 and addendum 2020-00267), the Erasmus MC Ethics Committee (MEC-2018-1183), the Privacy Committee of the Nationwide Network and Registry of Histopathology and Cytopathology (PALGA). We included 535 SLNB-negative patients ≥18 years treated for cutaneous melanoma at the Sahlgrenska University Hospital (2006 - 2014) and Erasmus MC Cancer Institute (2007 - 2017). Exclusion criteria were multiple primary melanomas, missing data regarding age or Breslow thickness, insufficient FFPE material from the primary tumor, and failed quality control of the quantitative polymerase chain reaction (qPCR). The cases were reviewed and re-staged according to AJCC version 8 staging system.

3.1.4 PAPER IV

Ethical approval for the study was rendered by the Swedish Ethical Review Authority (Dnr 908-14, 2020-00267, 477-18, and 2021-02315). We selected the patients from two different cohorts, based on the disease course after the excision of the primary melanoma: (I) patients in a stable clinical stage IIa-IIc until the end of follow up in June 2022, who underwent sentinel lymph node biopsy (SLNB) between 2006 and 2014, at the Sahlgrenska University Hospital, Gothenburg, Sweden; and (II) patients operated for melanoma brain metastasis at the Sahlgrenska University Hospital between 2013 and 2019, previously diagnosed with a single primary cutaneous melanoma between 1992 and 2015. All patients were treatment-naïve prior to surgery of the primary tumor. Only patients with available tissue blocks containing sufficient tumor material from both brain metastases and primary tumors were included in the "brain metastasis cohort" (II), resulting in 21 patients. In the second step, 21 control patients with T3-T4 melanomas (I), matched for age and gender were identified within the Sahlgrenska SLNB cohort.

3.2 TISSUE COLLECTION

3.2.1 PAPER I

Full-skin tumor biopsies (1 mm in diameter) were collected under guidance of dermoscopy, by specially trained dermatologists from the clinically suspected melanomas immediately after the excision of the tumor, thereafter snap frozen

and stored at −80°C. All melanocytic tumors were studied preoperatively according to standard dermoscopic algorithms(138, 139). The clinical examination and the dermoscopic view guided the involved investigator to where the suspected melanoma might be thickest or most "aggressive"-looking. This part of the lesion must be avoided from biopsy prior to histologic examination. This step is a deliberate departure from current praxis and instructions in the national guidelines for handling of melanocytic tumors and requires a close co-operation with the diagnosing dermatopathologists, so that diagnostics of the primary lesion is not compromised. Additionally, one thick, locally advanced primary melanoma in chronic sun-damaged skin was biopsied to generate five primary tumor fragments (PT) and seven in-transit metastases (IT). The biopsies were immediately stored at −80°C. Normal skin from the vicinity of the primary tumor was used as a control.

3.2.2 PAPER II AND III

The primary tumor material used in the study was formalin-fixed paraffin embedded tissue retrieved from the archival blocks. The blocks were cut on a rotary microtome under rigorous RNase-free conditions and prevention of RNA contamination between the cases. The microtome knife was changed for every block, and the whole cutting instrument was cleaned. We selected representative blocks with the deepest tumor to produce 4 μm sections for routine hematoxylin and eosin (H&E) staining and five 10 μm section for RNA extraction. All cases were reviewed histologically using both archival (if available) and novel H&E slides. In case of discrepancy with the original report, the latest reviewer´s diagnosis became decisive. The 10 μm sections dedicated for RNA were kept refrigerated and shipped in 1.5 ml sterile Eppendorf tubes to SkylineDx (Rotterdam, the Netherlands) for RNA extraction and qPCR analysis. The samples were anonymized and blinded concerning SLNB outcomes. Tumor RNA was extracted from whole sections present in the tubes without macrodissection.

3.2.3 PAPER IV

All material used in this study consisted of archival formalin-fixed paraffin-embedded (FFPE) tissue blocks with excised primary cutaneous melanoma. The tumor blocks were obtained from pathology biobanks in Western Sweden , and cut to 4 μm consecutive sections for routine hematoxylin and eosin (H&E) staining and immunohistochemical stains. Diagnosis of melanoma, including tumor characteristics, were reviewed for all primary tumors and brain metastases. Patients without representative or insufficient residual tumor in the archival material were excluded.

3.3 NUCLEIC ACID EXTRACTION AND SEQUENCING

3.3.1 PAPER I

NUCLEIC ACID EXTRACTION

From the 1mm biopsies stored in -80ºC, tumor tissue was hurriedly separated from adjacent dermis or subcutaneous fat using sterile scalpel and magnifying glass. The tissue was homogenized using a Tissue Lyser (Qiagen), followed by DNA and RNA extraction using the All Prep DNA/RNA Mini Kit (Qiagen). RNA quality was controlled by Agilent Bioanalyzer 2100 (Agilent). Only samples with RIN >6 were included.

NGS, TARGETED GENE SEQUENCING AND WHOLE EXOME SEQUENCING

The haploid human genome contains 23 chromosomes with approximately 3 x 10^9 base pairs and 30 x 10^3 genes. The genes within human nuclear DNA encode for proteins and are organized as exons and introns. After transcription, introns are removed from the RNA transcript by splicing to generate the mature mRNA. We analyzed the genetic material from the tumors using several techniques, covering selected parts of the genome.
NGS (Next generation sequencing) has completely revolutionized the genome analysis. With NGS, the entire human genome may be sequenced in just one

day. NGS encompasses several sequencing techniques that allow a rapid broad investigation of the whole genome, exome or transcriptome through simultaneous sequencing of millions of clusters, or a detailed deep study of a small part of the DNA but at a high resolution. The common NGS method is based on initial clonal amplification of oligonucleotides with cluster generation and sequencing by synthesis (SBS) principle. During sequencing, one base with a fluorescent terminator is added at a time. The fluorescent agent is excited by laser and the signal is recorded. The four bases are labeled with four different fluorescent dyes and the genetic code is read step-by step cluster-wise. Millions of reads are generated in a parallel fashion and the technique requires analysis with bioinformatics through alignment to the reference genome.

Targeted sequencing (ultra-deep mode) covered 40 selected genes and was performed using TruSeq Custom Amplicon Low Input workflow and NextSeq500 (Illumina). A mean coverage of 5,758× was achieved (838 x – 12,958x). PT1 and IT3 were excluded from the dataset due to low mutant allele frequency. Targeted sequencing examines selected parts of the selected genes, allowing for a sensitive identification of somatic mutations in cancer-related genes.

Whole exome sequencing (WES) covering the protein coding part of the DNA was performed on the DNA samples from the tumor and matched normal DNA from the CSD^{high} case. The samples were sequenced using a HiSeq 2500 or NextSeq. Median target coverage was 68x – 126x. WES uncovers genetic variants within all exons of the genome(140).

RNA SEQUENCING

This technique enables investigation of the transcribed RNA molecules. RNA was isolated and purified, and in the next step used for synthesizing cDNA that to be sequenced by NGS. RNA-seq was performed on all samples from the CSD^{high} case, including tumor and normal tissue(141).

3.3.2 PAPER II AND III

QUANTITATIVE POLYMERASE CHAIN REACTION (qPCR)

Tumor cell RNA was isolated from histological tissue sections without previous macrodissection (142). RNA extraction was performed using the RNeasy FFPE kit and QIAcube (Qiagen, Hilden, Germany). The resulting RNA fragments >70 nucleotides were reverse transcribed into cDNA using the SuperScript VILO Master Mix (Thermofisher, Waltham, MA, USA). Gene expression levels were measured by q-PCR using SYBR-green chemistry (PowerUp™ SYBR™ Green Master Mix, Thermofisher). Amplification was performed using a QuantStudio 5Dx qPCR instrument (Thermofisher, Waltham, MA, USA) with 7.5 µl diluted cDNA as input per reaction. Each sample was measured as a single sample using 20 µM of forward and reverse primers. Each run was added a 1:100 diluted human reference cDNA sample obtained from Agilent (human reference RNA, Agilent Cat. No. 750500) and a negative (no cDNA) control. Cycle threshold (Ct) values were calculated automatically using a fixed threshold for the fluorescent signal for individual gene. The Ct values for the target genes (GDF15, CXCL8, LOXL4, TGFBR1, ITGB3, PLAT, SERPINE2 and MLANA) were normalized to the Ct-value average of two housekeeping genes RLP0 and beta-actin, yielding the ΔCt.

To calculate the CP-GEP probability score, the ΔCt values were added to additional clinicopathologic data: Breslow thickness and age, both included as linear related continuous variables. This data was used as input for the logistic regression model. The CP-GEP model generates a binary output: CP-GEP High Risk and CP-GEP Low Risk. Patients whose CP-GEP score was higher than the predefined cut-off value of 0.063 were considered High Risk, whereas the remaining were regarded as Low Risk.

3.4 STATISTICAL ANALYSIS

3.4.1 PAPER I

R was used for all statistics, the tests were non-parametric. The p-value was calculated using Wilcoxon signed-rank test and $p < 0.05$ was considered statistically significant.

3.4.2 PAPER II

All statistical analyses concerning the test performance were done using IBM SPSS Statistics (version 26) and R (version 3.6.1). The CP-GEP model rendered binary results, either high-risk or low-risk for SLN metastasis. To calculate the accuracy of the test, the SLN outcome was used as the gold standard, also in a binary fashion, either SLN positive or SLN negative. All patients had clinically negative nodes prior to SLNB. SLN metastases regardless size were considered as positive lymph nodes. Sensitivity, specificity, negative predictive value (NPV), and positive predictive value (PPV) were calculated for the various T stages. Percentage of patients classified as CP-GEP Low Risk was presented as the "SLNB reduction rate" (SLNB-RR).

Additionally, the CP-GEP model was compared to existing on-line nomograms that had been constructed for the same purpose, the MIA and MSKCC nomograms. Of note is that the two alternative nomograms do not provide a binary risk estimate, whereas CP-GEP has a fixed cut-off. To create comparable conditions, a cut-off of 5% was set for the online nomograms to binarize the risk probabilities which would most likely meet the clinical decisions according to the NCCN guidelines(143).

CP-GEP MODEL IN PAPER II and III

The CP-GEP test is a hybrid test with the input of clinical and histopathological parameters (patient´s age and Breslow thickness), and the expression of eight target genes in the FFPE primary cutaneous melanoma (ITGB3, PLAT, SERPINE2, GDF15, TGFBR1, LOXL4, CXCL8, and MLANA) using qPCR and the ΔCt method (105). For each patient, the CP-GEP score was rendered as either low risk or high risk based on a cut-off value of 0.063. The model was originally developed by Bellomo et al. for calculating of the risk of clinically occult sentinel lymph node metastasis of any size and number(105).

3.4.3 PAPER III

In this study, the CP GEP test with the same input of parameters as in paper II was evaluated with regards to 5-year recurrence-free survival (RFS) as a primary endpoint. The study cohort was enlarged by fusion of eligible patients from the Swedish and Dutch cohorts from previous studies. All patients with stage I–II melanoma from the Swedish and Dutch cohorts were included (106, 142). RFS was calculated from the excision of primary melanoma until the last

follow-up visit, death or first metastasis. Distant metastasis-free survival (DMFS) was calculated from the excision of primary melanoma to the last follow-up visit, death or first distant metastasis. Metastases beyond the regional lymph nodes were considered as distant metastases. Overall survival (OS) was established from the time of excision of primary melanoma to the last follow-up visit or death. For the Swedish part of the cohort originating from the Sahlgrenska University Hospital, the patients were continuously followed clinically after SLNB and the mortality data were obtained from the Swedish Cause of Death Registry. For the Dutch patients from Erasmus MC Cancer Institute, data on metastases were gathered from medical journals and PALGA registry. Mortality data were retrieved from The Netherlands Cancer Registry (NCR). Additionally, for patients in stage I and II we compared the CP-GEP results with the EORTC nomogram to predict the risk of recurrence. in patients with a negative SN (stage I/II) (144).
Kaplan–Meier curves regarding 5-year RFS, DMFS, and OS were constructed using the binary output of the CP-GEP test. Hazard ratio (HR) was calculated using a Cox proportional hazard regression model. The p-value<0.05 was considered statistically significant. For comparison with the EORTC nomogram in stage I and II patients(145), the input of clinical and histopathological parameters Breslow thickness, ulceration and anatomical site generated three prognostic EORTC risk groups: low, intermediate and high. Patients without data on ulceration and/or primary tumor site were excluded. Analyses were performed using R version 3.6.1 (R Core Team, Vienna, Austria; 2021), gtsummary R package (version 1.3.3) and survminer (version 3.1.8 and version 0.4.6) R packages.

3.4.4 PAPER IV

Statistical analyses for calculating the differences between the cohorts were performed using IBM SPSS Statistics (version 28.0.1.0) and R (version 3.6.1). Statistical testing for differences between groups was non-parametric (two-sided Mann-Whitney test and Chi square test).

3.5 IMMUNOHISTOCHEMISTRY

3.5.1 PAPER IV

4 µm sections from the archival FFPE tumor were pretreated using a Dako PT-Link with EnVision FLEX Target Retrieval Solution (high pH). Dako

Autostainer Link 48 with EnVision FLEX reagents (DakoCytomation, Glostrup, Denmark).

were utilized for immunohistochemistry.

Primary antibodies used for immunohistochemistry were:

Mouse anti-CD8 (ready-to-use, IR623, Dako, Glostrup, Denmark)
Mouse anti-CD20 (ready-to-use, IR604, Dako, Glostrup, Denmark)
Mouse anti-BCL2 (ready-to-use, IR614, Dako, Glostrup, Denmark)
Mouse anti-BCL6 (ready-to-use, IR625, Dako, Glostrup, Denmark)
Mouse anti-CD138 (ready-to-use, IR642, Dako, Glostrup, Denmark)
Mouse anti-Ki67 (ready-to-use, IR626, Dako, Glostrup, Denmark)
Mouse anti-CD23 (ready-to-use, IR781, Dako, Glostrup, Denmark)
Mouse anti-SOX10 (ready-to-use, BC-API3099H, Biocare Medical, Pacheco, CA, USA). Magenta chromogen.

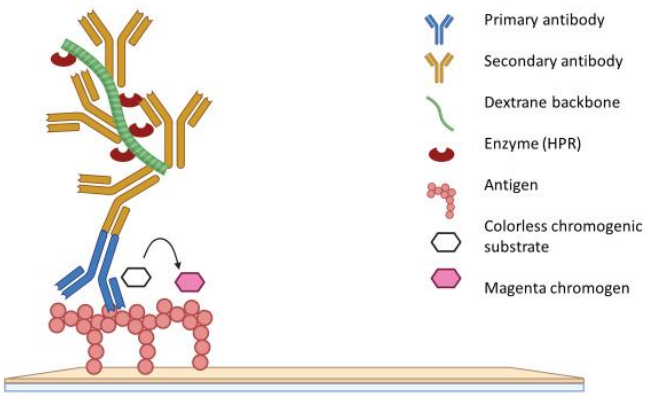

Figure 11. Principles of indirect immunohistochemistry. Abbreviation: HPR, horse-radish peroxidase. Created with Biorender.com

3.6 DIGITAL IMAGE ANALYSIS

3.6.1 PAPER IV

The whole tissue immune stained slides were scanned at 40x magnification (Hamamatsu NanoZoomer S210. The study cases were blinded for patient

outcome during analysis using image analysis software from Visiopharm version 2021.09.1.10842. The image analysis application was trained to count cells with nuclei and cytoplasm of a specific size and color intensity. The color intensity level was fine-tuned to include the visually verified positive cells and excluded the non-specifically stained subjects. The analysis was performed for both CD8+ and CD20+ lymphocytes with magenta chromogen. CD8+ T lymphocytes and CD20+ B lymphocytes were counted around the deep invasive margin of the primary tumor. The region of interest (ROI) was defined individually for every tumor and the number of lymphocytes per mm^2 was calculated for each cell type, (Fig. 13). ROI for CD8+ cells included the deep portion of the tumor and the infratumoral stroma in equal proportions. ROI for CD20+ cells included the immediate infratumoral stroma. Each tumor was evaluated twice, and a mean count of the cellular density was calculated. In addition, the tertiary lymphoid structures (TLS) were counted and evaluated regarding their spatial distribution in association with the deep invasive tumor border.

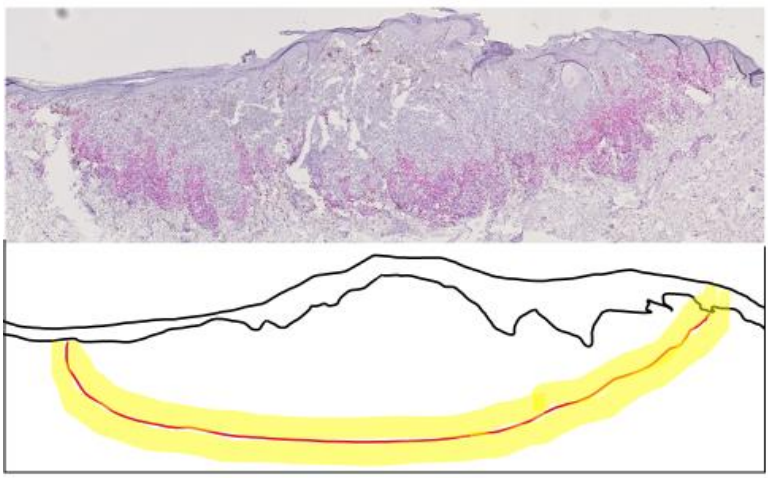

Figure 12. H&E and CD8 immunohistochemistry. Example of ROI demarcation for counting of CD8+cells.

4 RESULTS

4.1 PAPER I

184 patients from tertiary dermatology clinics in Southern Sweden with melanocytic lesions highly suspicious for melanoma or melanoma in situ were enrolled in this study. All tumors were completely excised and 72 were histologically diagnosed as melanoma in situ or invasive primary melanoma, constituting the study cohort. Tumors were categorized clinically as either CSD^{high} or CSD^{low}, based on anatomic site and age at diagnosis. 1 mm biopsies from each melanoma or melanoma in situ were further analyzed by ultra-deep targeted sequencing of 40 melanoma-relevant genes. Four categories of tumors were sequenced: CSD^{low} melanoma in situ (n=20), CSD^{low} melanoma (n=29), CSD^{high} melanoma in situ (n=13) and CSD^{high} melanoma (n=10).

BRAF and NRAS mutations were present in both types of melanoma

BRAF mutations were the most frequent mutations found in the entire cohort (n = 35, 49%); the majority were V600E (n = 20, 57%) with less frequent V600K (n = 7, 20%), K601E (n = 4, 11%), and complex hotspot mutations (T599dup and V600_K601delinsE). **BRAF** mutations were found in equal equal proportions among the CSD^{high} and CSD^{low} tumors (39% and 53%, respectively, p = .45), but the proportion of **V600K** mutations was higher (17%) in CSD^{high} vs 6% in CSD^{low} group. BRAF **V600E** was more common in the CSD^{low} group (39%) than in CSD^{high} (4%), in concordance with previous studies(146, 147). All **NRAS** (n = 13, 18%) were found in the Q61 codon, mutually exclusive to BRAF mutations. They were equally prevalent among the groups.

TERT promoter mutations were more frequent among the invasive CSD^{low} melanomas

We found frequent **TERT** promoter mutations in both histological types. Invasive CSD^{low} lesions demonstrated a higher frequency of TERT promoter mutations compared to in situ lesions (p = .002). Furthermore, we detected

three **KIT** -mutated cases (two CSD^{low} melanomas (V474A and T666L) and one CSD^{high} melanoma (L576P)). The former not present in COSMIC, suggesting a passenger role, while the latter found in 124 samples and suggested as pathogenic, indicating a driver role. Additionally, three **RAC1-mutated** cases in co-occurrence with BRAF or NRAS hotspot mutations, were identified.

In CSD^{high} melanoma, the mutational load is higher and BRAF V600K, NF1, and TP53 are frequently mutated

Mutations in **NF1** (n = 12, 17%) and **TP53** (n = 17, 24%) were more frequent in CSD^{high} as compared to CSD^{low} melanoma (NF1: 35% vs. 8%, p = .007; TP53: 48% vs. 12%, p = .002). Not surprisingly, there was a significantly higher **mutational load** in CSD^{high} compared to CSD^{low} lesions (p = .0048). In our cohort, this difference is most pronounced in the in-situ lesions of the two CSD type respectively (p = .008) than between the invasive subtypes (p = .16). Driver mutations within the two stages of the CSD^{high} melanomas were equally frequent, as was the extent mutational load (p = .93).

Mutational load is higher in invasive CSD^{low} melanoma compared to CSD^{low} in situ stage

The mutational load in invasive CSD^{low} lesions was higher than in the in situ forms (p = .05).

CSD^{high} melanoma reveals a high degree of similarity at the mutational, transcriptional, and copy number levels both within the primary tumor and in-transit metastases

One case of CSD^{high} primary tumor with multiple satellite and in-transit metastases was subjected to a triple molecular analysis to address the mutational and transcriptional heterogeneity in this entity. The patient presented clinically with a primary melanoma (PT) on the head and neck. Histological examination revealed a dense atypical spindled pigmented melanocytic proliferation in a background of severe solar elastosis and chronic inflammation in association with the tumor(148). Five regions of the primary tumor and seven synchronous in-transit metastases were analyzed by ultra-deep targeted sequencing, whole exome sequencing (WES) and RNA

sequencing. There were no differences in gene expression between the primary tumor and in-transit metastases. The specimens had a similar expression of the genes related to cell cycle, DNA repair, pigmentation, and immune responses. One PT and one IT sample showed high levels of antigen presentation and immune genes, due to dense inflammation. PT and IT specimens were similar concerning the expression of biologically important gene modules.

The **ultra-deep sequencing** with a median coverage (13,000×) discovered six mutations in cancer-related genes in all samples and one heterogeneous mutation (CTNNB1 P492S) confined to two PT samples and one IT.

Thereafter, **WES** was performed on the tumor samples, and the nearby normal skin sample, with an average target coverage of 68–126×. One PT and one IT sample were excluded due to low tumor purity. In total, we identified 1,844 somatically acquired mutations in all tumor specimens, including 1,819 SNVs, seven insertions, and 18 deletions. Of the SNVs, 163 (9%) were at adjacent genomic positions (DNVs, di-nucleotide substitutions), including 141 (87%) CC > TT substitutions, a feature of UV-related mutagenesis (149). 96% of the mutations, 1,774 were trunk mutations with **KIT** L576P and **CTNNB1** S33Y. Only 3.8% of the mutations were heterogeneously present between the samples (branch and private, or non-trunk) and the majority of these were considered passenger mutations. All samples exhibited a predominant UV-induced DNA damage signature(150).

We used WES data for the DNA copy number analysis. The aberration profiles were mostly similar, with gains and losses common to all samples. CDKN2A was lost exclusively in three IT. The otherwise ubiquitous copy number gain on chromosome 14 was absent from one PT and one IT.

4.2 Paper II

425 patients who underwent SLNB for primary cutaneous melanoma were included in the evaluation study of the CP-GEP test. Additional four cases were excluded, not fulfilling the quality control criteria for the detection of the housekeeping genes. After exclusion, 421 patients constituted the final study cohort. The median age was 60 years and 49% of the patients were females. Melanomas of head and neck were not present. The tumors originated most commonly from the skin of the trunk (48%) and leg (31%), displaying a median Breslow thickness of 1.8 mm. The majority of melanomas were T2 and T3 (50% and 28%, respectively) and ulceration was present in 32%. The most prevalent histologic types were WHO class I, CSD^{low} (SSM) melanoma (47%)

and nodular melanoma (39%). The overall SLN positivity in the study group was 13%.

The CP-GEP test classified 335 patients (80%) as CP-GEP High Risk and 86 (20%) as CP-GEP Low Risk for nodal metastasis. 83 of the 86 CP-GEP Low Risk patients (96.5%) were true negative patients, being SLNB negative. For T1-T2 patients, the negative predictive value (NPV) was 96.5% (95% CI: 90.0-99.3) and the SLNB reduction rate was 35.4% (95% CI: 29.4-41.8). Only one T3 and all T4 tumors were classified as CP-GEP High Risk. Patients ≥ 65 years and T1-T3 tumors (n = 171), had a SLNB reduction rate of 29.5% (95% CI: 22.1-37.8) with an NPV of 97.6% (95% CI: 87.1-99.9) (**Table 2 -4**).

	All samples n = 421	SN positive n = 54 (13%)	SN negative n = 367 (87%)	CP-GEP high n = 335 (80%)	CP-GEP low n = 86 (20%)
Gender, female	207 (49%)	26 (48%)	181 (49%)	164 (49%)	43 (50%)
Age at diagnosis (years), median (IQR)	60 (49–71)	57 (47–68)	61 (50–72)	60 (49–70)	62 (51–74)
Breslow (mm), median (IQR)	1.8 (1.3–3.2)	2.8 (1.8–4.3)	1.8 (1.3–3.0)	2.2 (1.5–3.6)	1.2 (1.1–1.4)
Ulceration, present	133 (32%)	27 (50%)	106 (29%)	117 (35%)	16 (19%)
pT stage					
T1	30 (7%)	1 (2%)	29 (8%)	14 (4%)	16 (19%)
T2	210 (50%)	19 (35%)	191 (52%)	141 (42%)	69 (80%)
T3	118 (28%)	18 (33%)	100 (27%)	117 (35%)	1 (1%)
T4	63 (15%)	16 (29%)	47 (13%)	63 (19%)	0 (0%)
Anatomical site					
Arm	87 (21%)	7 (13%)	80 (22%)	71 (21%)	16 (19%)
Trunk	202 (48%)	26 (48%)	176 (48%)	160 (48%)	42 (49%)
Leg	132 (31%)	21 (39%)	111 (30%)	104 (31%)	28 (32%)
Histologic type					
SSM	197 (47%)	17 (32%)	180 (49%)	138 (41%)	59 (69%)
LMM	7 (2%)	2 (4%)	5 (1%)	5 (2%)	2 (2%)
NM	165 (39%)	27 (50%)	138 (38%)	156 (47%)	9 (10%)
ALM	7 (2%)	3 (6%)	4 (1%)	4 (1%)	3 (3%)
Other/NOS	45 (11%)	5 (9%)	40 (11%)	32 (9%)	13 (15%)

Table 2. Patient characteristics. Abbreviation: SSM, superficial spreading melanoma;LMM, lentigo maligna melanoma; NM, nodular melanoma; ALM, acral lentiginous melanoma; NOS, not otherwise specified. (Reproduced with permission from Johansson I et al; Validation of a clinicopathological and gene expression profile model to identify patients with cutaneous melanoma where sentinel lymph node biopsy is unnecessary; EJSO 2022. Copyright, The Author(s)).

	pT1 n = 30	pT2 n = 210	pT3 n = 118	pT4 n = 63	pT1-T2 n = 240	pT1-T3 n = 358
CP-GEP high risk						
True positive	0	17	18	16	17	35
False positive	14	124	99	47	138	237
CP-GEP low risk						
True negative	15	67	1	0	82	83
False negative	1	2	0	0	3	3
PPV, % (95% CI)	0 (0–23.2)	12.1 (7.2–18.6)	15.4 (9.4–23.2)	25.4 (15.3–37.9)	11.0 (6.5–17.0)	12.9 (9.1–17.4)
NPV, % (95% CI)	93.8 (69.8–99.8)	97.1 (89.9–99.6)	100 (2.5–100)	–	96.5 (90.0–99.3)	96.5 (90.1–99.3)
SLNB-RR, % (95% CI)	53.3 (34.3–71.7)	32.9 (26.5–39.7)	0.8 (0–4.6)	0 (0–5.7)	35.4 (29.4–41.8)	24 (19.7–28.8)
Sensitivity, % (95% CI)	0 (0–97.5)	89.5 (66.9–98.7)	100 (81.5–100)	100 (79.4–100)	85.0 (62.1–96.8)	92.1 (78.6–98.3)
Specificity, % (95% CI)	51.7 (32.5–70.6)	35.1 (28.3–42.3)	1 (0–5.4)	0 (0–7.5)	37.3 (30.9–44.0)	25.9 (21.2–31.1)

Table 3. Performance metrics of the CP GEP model. Abbreviation: PPV, positive predictive value; NPV, negative predicitive value; SLNB RR, sentinel lymph node biopsy reduction rate. (Reproduced with permission from Johansson I et al; Validation of a clinicopathological and gene expression profile model to identify patients with cutaneous melanoma where sentinel lymph node biopsy is unnecessary; EJSO 2022. Copyright, The Author(s)).

Parameter	Definition	Calculation , Explanation
TP	True positive	CP GEP High risk and SLNB positive
TN	True negative	CP GEP Low risk and SLNB negative
FN	False negative	CP GEP Low risk and SLNB positive
FP	False positive	CP GEP High risk and SLNB negative
SY	Sensitivity	TP/(TP+FN)
SP	Specificity	TN/(TN+FP)
NPV	Negative predictive value	TN/(TN+FN)
PPV	Positive predictive value	TP/(TP+FP)
SLNB RR	SLNB reduction rate	(TN+FN)/(TP+TN+FN+FP)

Table 4. Overview of the performance metrics parameters.

Comparison with the MSKCC and MIA nomograms

The MSKCC nomogram is a on-line tool commonly used in the United States to guide SLNB decision making(94, 95). It utilizes five clinicopathologic variables: age, Breslow thickness, Clark level, primary tumor site and presence of ulceration. The MSKCC risk score could not be calculated for 20 patients (4.8%), due to Breslow depth > 10 mm (n = 5) or missing Clark level (n=16).

We also exposed our cohort for an Australian on-line nomogram tool available from MIA, aimed for prediction of the sentinel lymph node status(96, 98). This tool requires the input of the patient´s age, histologic subtype, Breslow thickness, ulceration, mitotic rate and lymphovascular invasion. MIA risk score could not be rendered for 45 of our patients (10.7%), due to discrepancies in valid histologic subtype. Also, mitotic count is not compulsory in the Swedish pathology reports for melanoma and could not be used for input in

	pT1-T3 n = 303		
	CP-GEP	**MSKCC**	**MIA**
PPV, % (95% CI)	12 (8.1–16.9)	11.5 (7.8–16.1)	10.3 (7.1–14.3)
NPV, % (95% CI)	95.7 (88–99.1)	96.1 (86.5–99.5)	100 (2.5–100)
SLNBRR, % (95% CI)	23.1 (18.5–28.3)	16.8 (12.8–21.5)	0.3 (0–1.8)
Sensitivity, % (95% CI)	90.3 (74.2–98)	93.5 (78.6–99.2)	100 (88.8–100)
Specificity, % (95% CI)	24.6 (19.6–30.2)	18 (13.6–23.1)	0.4 (0–2)

Table 5. Comparison of the performance of the CP- GEP model and the MSKCC and MIA nomograms. (Reproduced with permission from Johansson I et al; Validation of a clinicopathological and gene expression profile model to identify patients with cutaneous melanoma where sentinel lymph node biopsy is unnecessary; EJSO 2022. Copyright, The Author(s)).

the tool. Hence, the performance of MIA nomogram might be underestimated. MSKCC and MIA nomogram risk scores were established for 358 patients, of which 303 patients had pT1-T3 melanoma. The performances of the MIA, MSKCC and CP-GEP were calculated for comparison. In the pT1-T3 subgroup, CP-GEP demonstrated a SLNB reduction rate of 23.1%, compared to MSKCC 16.8% and MIA 0.3%. The NPV was 95.7% for the CP-GEP compared to MSKCC 96.1% and MIA 100% (**Table 5**).

We included 535 patients from Sweden and the Netherlands, all with stage I and II melanoma. Median age was 60 years, median Breslow depth of 1.8 mm, and ulceration was present in 28.4 %. The most prevalent stages were IB (42.2%) and IIA (27.7%) and 52.5% were SSM melanomas. The majority of the tumors were located on the trunk (47.9%), and the lower extremities (31.2%).

The 5-year recurrence-free survival (RFS) was 83.5%. The 5-year distant metastasis-free survival (DMFS) was 88.8% and 5-year overall survival (OS) 86.7%. 75.7% of the patients were followed for more than 5 years and 26.4% were followed up to 10 years after the PT diagnosis.

122 (22.8%) were classified as CP-GEP low-risk and 413 (77.2%) as CP-GEP high-risk. Subsequently, the patients were stratified by their CP-GEP test outcomes, resulting in a 5-year and 10-year RFS of 92.9% and 90.6% for the CP-GEP low-risk versus 80.7% and 74.9% for the CP-GEP high-risk patients ($p < 0.004$). HR 2.84, 95%CI 1.47–5.45, $p<0.002$.

The EORTC nomogram (151) classified 25% (n=130) of the patients in our cohort as a ‘low risk’ of recurrence (96.8% 5-year RFS). 49% (n=261) were ‘intermediate risk’ (88.4% 5-year RFS), and 26% (n=137) ‘high risk’ (**Figure 13**).

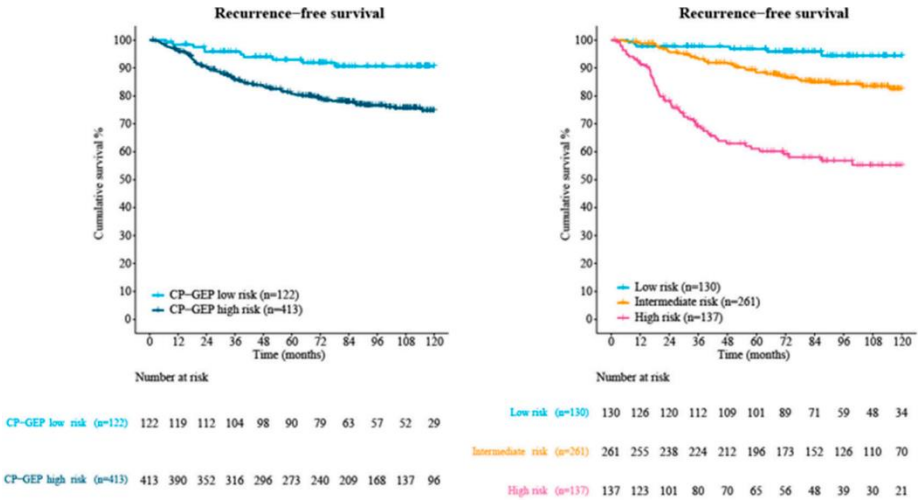

Figure 13. Recurrence-free survival in CP-GEP low risk and high-risk patients and MSKCC subgroups. Reproduced with permission from Johansson I et al; Using a Clinicopathologic and Gene Expression (CP-GEP) Model to Identify Stage I–II Melanoma Patients at Risk of Disease Relapse; Cancers 2022. Copyright, The Author(s)).

4.3 PAPER IV

In total, 42 patients were included in the study. All patients had undergone a complete excision of a single primary cutaneous melanoma. Of these patients, 21 had subsequently developed brain metastasis and were operated at the Sahlgrenska University Hospital; we assigned this group the" Brain metastasis" group. Availability of sufficient FFPE material from both primary tumor and brain metastasis was a limiting factor while identifying the study subjects for the "Brain metastasis" group. All eligible patients with the diagnosis of melanoma brain metastasis at the Sahlgrenska University hospital were included. 50% of the patients were women, and the median age at the diagnosis of the primary tumor was 61 years. Median Breslow depth was 2.3 mm, and 48% displayed ulceration, compared to Breslow 2.7 mm and 29% ulceration in the" Control" group. The" Control" patients were identified within the Sahlgrenska SLNB cohort, and consisted of 21 gender and age-matched patients with previous T3-T4 melanoma without evidence of recurrence or death until the end of follow-up. Patients in both groups were systemic treatment- naïve at the time of excision of the primary tumor. All patients in the" Control" group were alive by the end of the follow-up, and the median follow-up time in this group was 11.4 years (IQR 8.4-13.2). During follow-up, 16 patients (76%) in the" Brain metastasis" group had died of

melanoma, with a median time from the primary tumor diagnosis to death of 6.4 years (IQR 3.1-9.1).

Density of melanoma- associated CD8+ and CD20+ lymphocytes.

Primary melanoma tissue from archival FFPE blocks from 42 patients was stained with immunohistochemistry. Both CD8+ and CD20+ demonstrated a dominating infiltration within the deep invasive margin and adjacent infra-tumoral stroma. This interface area was chosen for the measurements of the cellular density of the lymphocytes. High densities of CD8+ T cells and CD20+ B cells in the deep invasive part of the primary melanoma, and the immediate infratumoral stroma were closely associated with good outcomes. Median densities of CD8+ T cells in the" Control" group were 4894 (IQR 3365-6388) and 1412 (IQR 498-2184) in the" Brain metastasis" group, there was a statistically significant difference between the two groups, $p<0.001$. Median densities of CD20+ were also statistically significantly higher in the" Control" group compared to the" Brain metastasis" group (1123 (IQR 503-2095) and 280 (IQR 120-402)), respectively ($p<0.001$).

Tertiary lymphoid structures

Early-stage tertiary lymphoid structures (TLS) were present in the infra-tumoral stroma in close association to the tumor-stromal interface. The highly mature forms of TLS characterized by germinal centers and high endothelial venules (HEV) were not observed in our material. TLS were present in 67% of the tumors in the" Control" group and 48% of the" Brain metastasis" group, the difference between group was not statistically significant. Four of the tumors within the" Control" group showed a distinct architectural pattern, " String of pearls" with TLS located in a linear fashion below the tumor, with equal distances between the individual cell clusters (**Figure 14**).

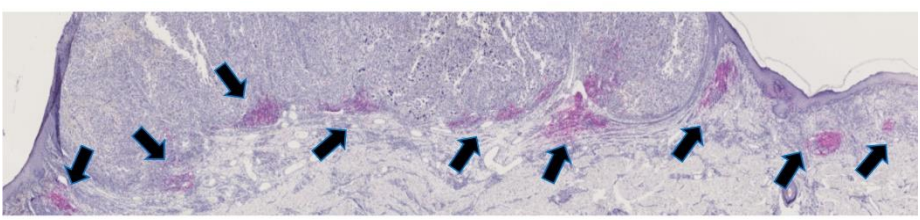

Figure 14. Nodular melanoma Breslow 3.3 mm, pT3a, without recurrence ("Control" group). TLS arranged as a String of pearls. CD20 immune stain. Arrows indicate the TLS.

Another distinct histological pattern was noted in one tumor in the “Control” group, displaying a diffuse infiltration of single B cells within the tumor and the infra-tumoral stroma, a” Snowfall pattern”, without formation of any TLS. The tumors in the” Brain metastasis” group did not show any of these two patterns in any tumor.

5 DISCUSSION AND CONCLUSIVE REMARKS

5.1 PAPER I

In this paper, we focused on the molecular features of the CSD^{high} melanoma, both in situ and invasive phases. Previous studies were primarily based on metastatic CSD^{low} melanoma(152-156). The study cohort contained both CSD^{high} and CSD^{low} melanoma, allowing for a comparison of these two entities.

Our results confirmed that the CSD^{high} melanoma contains more mutations than the CSD^{low} tumors(64, 152, 157) with a high frequency of NF1 and BRAF V600K mutations(146, 147). Ultra-deep sequencing did not reveal differences in mutation frequencies between in situ and invasive CSD^{high} melanoma. The technique was selected to allow the detection of melanoma-related mutations despite admixture with the normal surrounding tissue. We conclude that CSD^{high} melanoma acquires numerous oncogenic mutations already in the intraepidermal phase and may not need additional mutations to progress into the invasive phase. Epigenetic alterations and inferior immunologic responses may drive the transition of the intraepidermal to invasive dermal population. This process is probably rather slow, mainly resulting in broad colonization of the epidermis, as supported by the classical clinical description of lentigo maligna: a slowly growing pigmented macule located mainly on the face of fair-skinned elderly (i.e.CSD^{high} skin) individuals. In addition, some of the early invasive CSD^{high} lesions pose diagnostic problems for pathologists due to their resemblance to more benign dermal processes.

This data needs to be interpreted with some caution due to the fact that the epidermal keratinocytes in the CSD^{high} skin harbor a high number of UV-related mutations that may contribute to the overall high mutational load when analyzing the CSD^{high} melanoma in situ. Also, many of the detected mutations in the CSD^{high} melanoma may represent passenger mutations that do not result in an increased malignant capacity compared to the CSD^{low} melanoma.

On the other hand, CSD^{low} melanoma shows an accumulation of somatic mutation during progression from the in situ to the invasive phase, as reported previously(158).

We also investigated the tumor heterogeneity within one primary CSD^{high} tumor and its synchronous satellite and in-transit metastases. We found an

overall similarity in transcriptional and mutational patterns and DNA copy numbers as if a single lesion was analyzed. Macroscopically, the primary tumor was surrounded by a symmetrical scatter of small metastases, suggesting a central origo giving rise to off-springs with similar temporal and spatial kinetics. The tumors exhibited trunk mutations with a UV signature. On the other hand, the non-trunk mutations were less related to UV. Another feature was a heterogeneous loss of CDKN2A, suggesting subclonality associated with progression, as previously reported(64, 158)

To conclude, our analysis of CSD^{high} melanoma revealed a limited variation in mutational patterns and copy number changes during the transition from in situ to the invasive and the early metastatic phase. These findings suggest that the acquisition of mutations does not orchestrate early tumor progression in this subtype of melanoma. CSD^{low} and CSD^{high} melanoma are separate entities both histologically and biologically, with variations in the tumor-initiating events and progression.

Our case was deeply analyzed, and the results expand the knowledge of tumor heterogeneity of the early stages of CSD^{high} melanoma but is limited to one case. Continued investigation is necessary to unravel the true extent of heterogeneity within CSD^{high} tumors.

5.2 PAPER II

In Sweden, SLNB is most commonly meant for patients with >T1 melanoma. In paper II, we evaluated the CP-GEP model for the prediction of SLNB metastasis in a cohort of Swedish patients with primary cutaneous melanoma. Studies of melanoma in the Swedish population are fueled by the high incidence of cutaneous melanoma, the long tradition of standardized clinical management, including SLNB(159), as well as the population-based tumor registry with high coverage. After being developed in a patient cohort at the Mayo Clinic in the United States, the CP-GEP test was initially validated in an independent Dutch patient cohort at the Erasmus Medical Center in the Netherlands (EMC)(105, 142). Our results revealed a negative predictive value of 96.5% in pT1-T2 tumors and a possibility to reduce SLNB by 35.4%. Patients with thicker melanomas (T3 and T4) demonstrated less or no utility of the test as only one T3 tumor was classified as CP-GEP Low Risk (0.8%), and all pT4 tumors were classified as CP-GEP High Risk for sentinel lymph node metastasis. We conclude that the T2 subgroup benefits most from the test if the focus is the safe avoidance of SLNB in the case of CP-GEP low-risk results. SLNB is mainly offered to risk groups with an estimated SLNB positivity >

5%; in Sweden, primarily to patients with pT2-pT4 tumors, corresponding to 50% of primary cutaneous melanomas.

To compare the three patient cohorts, we found that the prevalences of the CP-GEP Low-Risk patients were similar in the two Swedish and Dutch cohorts (20%) but 40% in the Mayo cohort. We conclude that the differences in the prevalence of low-risk CP-GEP are based on the prevalence of pT1 melanoma in the three cohorts, EMC 4.8%, Sahlgrenska 7.1%, and Mayo 24.9%, as well as by the differences in pT4 tumors: EMC 16.7%, Sahlgrenska 15.0%, and Mayo 3.7%. In addition, SLNB positivity differed between the cohorts, in Sahlgrenska, with 13% positivity rate and a higher percentage in the Mayo and EMC cohorts, 19% and 29%, respectively. This variation in SLNB positivity rate may originate in true differences between the patient cohorts or the technical or methodological variation within lymphoscintigraphy, surgery, or pathology at the time of the biopsy. Melanomas of the head and neck region were not included in the Sahlgrenska cohort, and in the EMC cohort, only a few patients were.

SLNB is a resource-demanding procedure necessitating a multidisciplinary organization with anesthesiology, scintigraphy, surgery, and pathology. It constitutes a specific but poorly sensitive prognostic marker with negative findings in approximately 80% of the patients. SLNB may also cause iatrogenic harm to the patient (160, 161). Followingly, finding a safe alternative to SLNB may be beneficial both for the patients and healthcare providers.

According to National guidelines (122), the selection of the patients for SLNB is based on stage according to the AJCC version 8. Histologic parameters Breslow thickness and ulceration are crucial risk determinants. There are alternative ways to predict the risk of sentinel lymph node metastasis, such as online nomograms. We compared the results of the CP_GEP test with two nomograms from the MSKCC nomogram and the MIA and showed a similar NPV, but CP-GEP indicated a higher SLNB reduction rate in pT1-T3 patients. Among the patients ≥ 65 years with pT1-T3 melanomas, the NPV and SLNB reduction rates were even higher. To conclude, patients ≥ 65 years may benefit even more from the CP-GEP since they have a higher risk for SLNB complications.

To summarize, CP-GEP is a highly specific non-invasive method to identify patients at low risk for nodal metastasis and safely deselect them from the SLNB procedure, enriching the SLNB group for positive outcomes. In our

study cohort, 35.4% of the SLNB in the pT1-T2 group may have been safely unperformed due to the very low risk (144)of SLN metastasis.

5.3 PAPER III

SLNB positivity identifies 20% of patients at higher risk of disease recurrence and melanoma-specific mortality. The patients in stage IIIB-C are currently eligible for adjuvant systemic treatment (162-164). Nevertheless, >40% of the patients initially diagnosed with stage I–II melanoma, with or without SLNB investigation, will eventually experience disease recurrence or die of melanoma(165, 166). Melanoma-specific survival is comparable in patients with stage IIA–C and IIIA/B melanoma (93–83%) and (94–82%), respectively(167). There is a need for another prognostic marker beyond Breslow and ulceration for node-negative patients or those who do not undergo SLNB. In paper III, we combined Swedish and Dutch patient cohorts with negative SLNB and showed that the CP-GEP test could identify stage I-II patients with a high risk of recurrence and a lower 5-year RFS, DMFS, and OS.

Using the EORTC nomogram as a benchmark, the CP-GEP and EORTC nomograms resulted in comparable numbers of patients with a low risk of recurrence: 22.8% (122/535) and 24.6% (130/528), respectively. One crucial difference is that the EORTC nomogram requires an input of SLNB data, and the CP GEP test does not(144).

Examples of alternative tools for survival prediction are the Swedish prognostic instrument, MIA nomogram for thin melanoma, and 31-GEP assay.

The Swedish prognostic instrument needs the input of age, gender, tumor site, Breslow thickness, ulceration, Clark's level of invasion, and, when applicable, **SLNB status**(168). In this tool, Breslow thickness has the greatest prognostic impact; the presence of ulceration almost doubles, and a positive SN triples the risk of melanoma-specific mortality.

MIA prognostic instrument for thin melanoma uses age, gender, Breslow thickness, ulceration, melanoma subtype, tumor localization, **mitoses, and SLNB status** (100). Albeit, counting mitoses is problematic and often not reported.

A novel **GEP** presented by Thakur et al. has a prognostic value similar to the AJCC staging but with an added value in stage I melanomas (169).

The **31-GEP assay** (28 discriminating and three control genes, DecisionDx-Melanoma) has been evaluated in thin melanomas(103). During validation, the 31-GEP assay was a significant predictor of the RFS and DMFS in patients with stage I and II melanoma. The 31-GEP has been investigated in several studies (170-173), but its value for clinical use in thin melanomas still needs to be clarified(174).

The **11-GEP (MelaGenix)** assay (175) is a nine-gene signature assessing six protective genes KRT9, DCD, PIP, SCGB1D2, SCGB2A2, and COL6A6 and three risk genes KBTBD10, ECRG2, and HES6. Nevertheless, a systematic review and meta-analysis examining the use of 31-GEP and 11-GEP assays in stage I disease demonstrated disappointing results for both assays (176).

CAM-121 signature is another promising GEP utilizing the expression of 121 genes. It was developed using transcriptomic data from stage IIB and III melanoma in the AVAST-M study(177). The signature was externally validated in a patient cohort with I and IIA melanoma stages showing that this GEP is associated with melanoma-specific survival.

In paper II, we showed that the CP-GEP test is highly specific and could be utilized as a "rule-out" test to identify patients with pT1-T2 melanoma at low risk of recurrence and for whom SLNB could safely be forgone(106). Changing the indication of the CP GEP test to a "rule-in" test to identify patients at high risk of recurrence or melanoma-specific death requires further adjustments to the test algorithm.

The KEYNOTE-716 trial showed that pembrolizumab in the adjuvant setting might significantly prolong the recurrence-free survival in stage IIB/C patients (178). The desire to move adjuvant therapy to the earlier stages of melanoma urges the need for additional prognostic testing to better stratify the patients at high risk for recurrence.

Prediction of stage I melanoma is difficult due to the small number of events in this subgroup. It requires a very large sample size to stratify a study cohort by stage and gene expression analysis. No GEP tools are currently included in the NCCN guidelines® for melanoma (143). To evaluate the clinical utility of the novel tests in precision medicine, validation in independent cohorts, preferentially within the frame of prospective randomized trials, would be desirable(179).

Our results show that the prediction of survival using genetic information in primary melanoma combined with clinical and histological variables is

promising. However, the current CP-GEP algorithm labels the majority of the patients with stage I–II melanoma as having a high risk of disease recurrence. It would result in overtreatment if used for selecting stage I and II patients for adjuvant treatment. The test algorithm needs to be further adjusted by adding other histological, clinical, and gene expression variables to decrease the false positive rate.

5.4 PAPER IV

This study aimed to evaluate the utility of a limited immunohistochemical panel with digital quantification of immune cells as a biomarker in primary melanoma. We used FFPE primary melanoma material from two patient cohorts with 21 patients in each: 1. patients with thick T3 and T4 melanomas without recurrence on a long-term follow-up, and 2. patients whose melanomas metastasized to the brain, leading to rapid death in most of the cases. Clark has proposed tumor-infiltrating lymphocytes (TILs) as an independent prognostic factor for melanoma-specific survival(180, 181). Histologically assessed TILs have never been implemented broadly in clinics due to being poorly reproducible and labor-intensive. The original designation of the TILs concept was a semi-quantitative approach characterizing the presence of TILs as absent, present/non-brisk, or present/brisk. Although TILs are associated with better prognosis(182), their assessment is not a part of the current staging. The traditional histologic TILs evaluation has persisted so far despite the more nuanced approaches that came with various complex analyses of TILs subclasses, cell functional states, and gene expression(183, 184). Unfortunately, TILs assessment using categorical grading systems is poorly reproducible, where many cases become under- or overstaged, and alternative histologic approaches have been proposed to improve the reproducibility(185). The emergence of digital pathology may enhance the cell quantification and re-open for introduction of TILs in the routine evaluation of primary melanoma.

In our study, we selected CD8+ T lymphocytes and CD20+ B lymphocytes associated with primary melanoma for quantification. CD8+ cells are crucial effector cells specifically targeting melanoma cells with cytotoxic actions. B cells´ roll in the tumor microenvironment of primary melanoma is more complicated, with both pro- and anti-inflammatory effects. The role of tumor-associated B cells in melanoma is essential for sustaining inflammation(186). In the primary follicles, naive B cells recognize the tumor antigens and move toward the edge of the follicle to connect with the activated CD4+ and CD8+

T cells that have the same antigen specificity. The activated B cells may differentiate into immunoglobulin-producing plasma cells, others proliferate and form germinal centers within lymph nodes, and yet others target the primary tumor site to form tertiary lymphoid structures. As previously shown in metastatic melanoma, co-localization of both CD20+ cells and CD8+ cells is beneficial for the anti-tumoral cytotoxic action of CD8+ T cells. (115).

The results of our study showed significant differences between CD8+ and CD20+ cell densities in the tumor-stromal interface. Low densities of both CD8+ and CD20+ cells pointed towards a dismal prognosis and risk of brain metastasis, as indicated by the composition of the cohorts.

TLSs were present in both cohorts, but the difference was not significant. Nevertheless, we made a previously undescribed observation regarding the architectural pattern of distribution of TLS: in the" Control"group, we identified four tumors with TLS organized in an orderly linear pattern at equal distances from each other, reminiscent of a "string of pearls", as well as one tumor with an unusual diffuse intratumoral B cell infiltration "a snowfall pattern". None of these distinctive patterns were observed in the" Brain metastasis" group. These findings indicate a better outcome and should be investigated in a larger cohort.

The major limitation of this study is the fact that the cohorts were matched for age and gender, not for primary prognostic factors, Breslow thickness, and ulceration. Also, the size of the study cannot result in any absolute cut-off value. A more extensive study including stratified patient groups with various outcomes would be beneficial. Another limitation is that metastatic spread of melanoma commonly occurs at extracranial sites, and this category of patients was not included.

6 FUTURE PERSPECTIVES

We are in the era of a *paradigm shift* concerning cancer diagnostics, treatment, and follow-up. Nuancing the diagnosis of primary melanoma and fine-tuning prognostication of melanocytic tumors within the frames of personalized medicine has been fueled by the advent of effective but costly and potentially harmful therapies. Due to numerous clinical trials with promising outcomes, systemic treatments have become available to a growing group of patients.

Histopathological evaluation has so far kept the position of a gold standard for the diagnosis and prognosis of melanocytic tumors. However, it is becoming more and more apparent that the best approach encompasses the *integration* of histologic, clinical, immunological, and molecular features that cover the essential aspects of melanomagenesis and tumor progression.

The fast-growing field of novel laboratory, imaging, and digital techniques will generate new biomarkers to tailor the individual patient treatment and follow-up strategies. The development of GEP tests is highly attractive due to their reproducibility and non-invasive approach. Also, the characterization of tumor microenvironment with translational applications is highly promising. With the current developmental pace of melanoma treatment and diagnostics in mind, close to zero melanoma mortality is achievable, especially in combination with the prevention and early detection of melanoma.

7 ACKNOLEDGEMENTS

Many people have contributed to the creation of this thesis.

I would like to express my deepest gratitude to **Lars Ny**, my main supervisor, without you and **Roger Olofsson Bagge,** my main co-supervisor, this thesis would never be completed. Thank you from the bottom of my heart for all your support, encouragement, sharing your clinical experience and knowledge of science with me. **Jan Mattsson**, for your kind support of my work with the outstanding patient database initiated and maintained by you since 2006.

Göran Jönsson, my former main supervisor from the beginning of my PhD studies at the University of Lund, for introducing me to the world of serious science and for sharing your deep knowledge of melanoma genomics.

Levent Akyurek, Dimitrios Katsarelias, Henri Puttonen, Karin Jirström, my present and former co-supervisors and colleagues in Lund and Gothenburg, Christian Ingvar, Gustav Christensen, Irina Baranovskaya, Kari Nielsen and other members of Lund Melanoma Study Group for your friendship, support and sharing your expertise in melanoma research.

David Elder, Peggy Elder and members of the International Melanoma Pathology Study Group for kindly sharing your profound knowledge of melanoma pathology, being good friends and amazing role models.

My co-authors, **Adriana, Katja, Gustav, Martin, Shamik, Frida, Jan, Barbara, Dennie, Evalyn, Jvalini, Anna, Henrik**.

Helge Löfberg and Otto Ljungberg, my colleagues from the Department of Pathology in Malmö who introduced me to pathology during my residency, kindly sharing your professional excellence and letting me understand that dermatopathology is so fascinating.

Åse Silverdal, my closest colleague, simultaneously exposed for PhD students both at home and work, for all your substantial support while I focused on this thesis. **Lena Mölne, Jan Siarov, Noora Neittanmäki, Christina Jensen**, my dermpath colleagues at the Department of Clinical Pathology, for running the diagnostics during my PhD studies.

Ellinor Matsson, Gulay Altiparmak, and the great lab technician team at Sahlgrenska for your dedicated support and indispensable practical help with the laboratory work.

Anders Bergström, Magnus Hansson and Michael Wilstermann, my colleagues within the management team at the Departement of Pathology, Sahlgrenska University Hospital for being emotionally and practically supportive, taking over my part of the job while I was finalizing this thesis.

Christina Månsson for the life- saving help with statistics when I needed you the most.

My mom **Iva and dads Zdenek and Jiri**, and cousin **Jirka with family** for your unconditional love, guidance and support through all my life.

My wonderful children **Agnes, Iris, Ingrid and Astrid** for being patient and supportive during my long PhD period.

And lastly, **Martin**, my husband and my eternal everything, there are no words that could describe how much I love you.

8 APPENDIX

PAPER II and III

Real-life examples from the Sahlgrenska patient cohort

Patient 1: Male 62, SSM melanoma on the back, Breslow thickness 1.4 mm, no ulceration, pT2a. Follow up: SLNB negative, no recurrence

Skyline CP-GEP:	low risk
MIA:	12 % risk of positive SLNB
MSKCC:	10% risk of positive SLNB
Swedish prognostic instrument:	5 years MSS 94-96%
	10 years MSS 84-89%
EORTC:	5 years recurrence risk 10.78%
	5 years MSS 95.59 %

Patient 2: Male 40, nodular melanoma on the back, Breslow thickness 2.7 mm, no ulceration, pT3a. Follow up: SLNB negative, no recurrence

Skyline CP-GEP:	high risk
MIA:	25% risk of positive SLNB
MSKCC:	24% risk of positive SLNB
Swedish prognostic instrument:	5 years MSS 91-94%
	10 years MSS 79-84%
EORTC:	5 years recurrence risk 17.45%
	5 years MSS 92.3%

9 REFERENCES

1. Cabrera R, Recule F. Unusual Clinical Presentations of Malignant Melanoma: A Review of Clinical and Histologic Features with Special Emphasis on Dermatoscopic Findings. Am J Clin Dermatol. 2018;19(Suppl 1):15-23.
2. Cancer IAfRi. GLOBOCAN 2020.2021 2022 [Available from: https://gco.iarc.fr/.
3. Aitken JF, Youlden DR, Baade PD, Soyer HP, Green AC, Smithers BM. Generational shift in melanoma incidence and mortality in Queensland, Australia, 1995-2014. Int J Cancer. 2018;142(8):1528-35.
4. Whiteman DC, Green AC, Olsen CM. The Growing Burden of Invasive Melanoma: Projections of Incidence Rates and Numbers of New Cases in Six Susceptible Populations through 2031. J Invest Dermatol. 2016;136(6):1161-71.
5. SweMR - Svenska Melanomregistret. Nationell årsrapport för hudmelanom,. 2019.
6. Carlino MS, Larkin J, Long GV. Immune checkpoint inhibitors in melanoma. Lancet. 2021;398(10304):1002-14.
7. Rathod D, Kroumpouzos G, Lallas A, Rao B, Murrell DF, Apalla Z, et al. Critical Review of the Sentinel Lymph Node Surgery in Malignant Melanoma. J Drugs Dermatol. 2022;21(5):510-6.
8. Brito FC, Kos L. Timeline and distribution of melanocyte precursors in the mouse heart. Pigment Cell Melanoma Res. 2008;21(4):464-70.
9. Price ER, Fisher DE. Sensorineural deafness and pigmentation genes: melanocytes and the Mitf transcriptional network. Neuron. 2001;30(1):15-8.
10. Goldgeier MH, Klein LE, Klein-Angerer S, Moellmann G, Nordlund JJ. The distribution of melanocytes in the leptomeninges of the human brain. J Invest Dermatol. 1984;82(3):235-8.
11. Zecca L, Tampellini D, Gatti A, Crippa R, Eisner M, Sulzer D, et al. The neuromelanin of human substantia nigra and its interaction with metals. J Neural Transm (Vienna). 2002;109(5-6):663-72.
12. Vandamme N, Berx G. Melanoma cells revive an embryonic transcriptional network to dictate phenotypic heterogeneity. Front Oncol. 2014;4:352.
13. Green SA, Simoes-Costa M, Bronner ME. Evolution of vertebrates as viewed from the crest. Nature. 2015;520(7548):474-82.
14. Jin EJ, Erickson CA, Takada S, Burrus LW. Wnt and BMP signaling govern lineage segregation of melanocytes in the avian embryo. Dev Biol. 2001;233(1):22-37.

15. Takeda K, Yasumoto K, Takada R, Takada S, Watanabe K, Udono T, et al. Induction of melanocyte-specific microphthalmia-associated transcription factor by Wnt-3a. J Biol Chem. 2000;275(19):14013-6.
16. Levy C, Khaled M, Fisher DE. MITF: master regulator of melanocyte development and melanoma oncogene. Trends Mol Med. 2006;12(9):406-14.
17. Potterf SB, Furumura M, Dunn KJ, Arnheiter H, Pavan WJ. Transcription factor hierarchy in Waardenburg syndrome: regulation of MITF expression by SOX10 and PAX3. Hum Genet. 2000;107(1):1-6.
18. Tachibana M, Kobayashi Y, Matsushima Y. Mouse models for four types of Waardenburg syndrome. Pigment Cell Res. 2003;16(5):448-54.
19. Adameyko I, Lallemend F, Furlan A, Zinin N, Aranda S, Kitambi SS, et al. Sox2 and Mitf cross-regulatory interactions consolidate progenitor and melanocyte lineages in the cranial neural crest. Development. 2012;139(2):397-410.
20. Ueno M, Aoto T, Mohri Y, Yokozeki H, Nishimura EK. Coupling of the radiosensitivity of melanocyte stem cells to their dormancy during the hair cycle. Pigment Cell Melanoma Res. 2014;27(4):540-51.
21. Lister JA, Capper A, Zeng Z, Mathers ME, Richardson J, Paranthaman K, et al. A conditional zebrafish MITF mutation reveals MITF levels are critical for melanoma promotion vs. regression in vivo. J Invest Dermatol. 2014;134(1):133-40.
22. de Vries TJ, Trancikova D, Ruiter DJ, van Muijen GN. High expression of immunotherapy candidate proteins gp100, MART-1, tyrosinase and TRP-1 in uveal melanoma. Br J Cancer. 1998;78(9):1156-61.
23. Nathan P, Hassel JC, Rutkowski P, Baurain JF, Butler MO, Schlaak M, et al. Overall Survival Benefit with Tebentafusp in Metastatic Uveal Melanoma. N Engl J Med. 2021;385(13):1196-206.
24. Du J, Miller AJ, Widlund HR, Horstmann MA, Ramaswamy S, Fisher DE. MLANA/MART1 and SILV/PMEL17/GP100 are transcriptionally regulated by MITF in melanocytes and melanoma. Am J Pathol. 2003;163(1):333-43.
25. Steeb T, Wessely A, Petzold A, Kohl C, Erdmann M, Berking C, et al. c-Kit inhibitors for unresectable or metastatic mucosal, acral or chronically sun-damaged melanoma: a systematic review and one-arm meta-analysis. Eur J Cancer. 2021;157:348-57.
26. Fitzpatrick TB, Breathnach AS. [the Epidermal Melanin Unit System]. Dermatol Wochenschr. 1963;147:481-9.
27. Teofoli P, Motoki K, Lotti TM, Uitto J, Mauviel A. Propiomelanocortin (POMC) gene expression by normal skin and keloid fibroblasts in culture: modulation by cytokines. Exp Dermatol. 1997;6(3):111-5.
28. Millington GW. Proopiomelanocortin (POMC): the cutaneous roles of its melanocortin products and receptors. Clin Exp Dermatol. 2006;31(3):407-12.

29. Raffin-Sanson ML, Ferre F, Coste J, Oliver C, Cabrol D, Bertagna X. Pro-opiomelanocortin in human pregnancy: evolution of maternal plasma levels, concentrations in cord blood, amniotic fluid and at the feto-maternal interface. Eur J Endocrinol. 2000;142(1):53-9.
30. Eijmael M, Janmaat CJ, Briet-Schipper EMN. [The risks of tanning with the Barbie drug]. Ned Tijdschr Geneeskd. 2022;166.
31. Langendonk JG, Balwani M, Anderson KE, Bonkovsky HL, Anstey AV, Bissell DM, et al. Afamelanotide for Erythropoietic Protoporphyria. N Engl J Med. 2015;373(1):48-59.
32. D'Alba L, Shawkey MD. Melanosomes: Biogenesis, Properties, and Evolution of an Ancient Organelle. Physiol Rev. 2019;99(1):1-19.
33. Ito S, Wakamatsu K. Quantitative analysis of eumelanin and pheomelanin in humans, mice, and other animals: a comparative review. Pigment Cell Res. 2003;16(5):523-31.
34. Jimbow K, Hua C, Gomez PF, Hirosaki K, Shinoda K, Salopek TG, et al. Intracellular vesicular trafficking of tyrosinase gene family protein in eu- and pheomelanosome biogenesis. Pigment Cell Res. 2000;13 Suppl 8:110-7.
35. Unver N, Freyschmidt-Paul P, Horster S, Wenck H, Stab F, Blatt T, et al. Alterations in the epidermal-dermal melanin axis and factor XIIIa melanophages in senile lentigo and ageing skin. Br J Dermatol. 2006;155(1):119-28.
36. Watanabe T, Tahira M, Morino S, Horie T, Adachi K, Tsutsumi R, et al. Novel morphological study of solar lentigines by immunohistochemical and electron microscopic evaluation. J Dermatol. 2013;40(7):528-32.
37. D'Arcy C, Kiel C. Cell Adhesion Molecules in Normal Skin and Melanoma. Biomolecules. 2021;11(8).
38. Hendi A, Wada DA, Jacobs MA, Crook JE, Kortuem KR, Weed BR, et al. Melanocytes in nonlesional sun-exposed skin: a multicenter comparative study. J Am Acad Dermatol. 2011;65(6):1186-93.
39. Whiteman DC, Parsons PG, Green AC. Determinants of melanocyte density in adult human skin. Arch Dermatol Res. 1999;291(9):511-6.
40. Haass NK, Herlyn M. Normal human melanocyte homeostasis as a paradigm for understanding melanoma. J Investig Dermatol Symp Proc. 2005;10(2):153-63.
41. Yamaguchi Y, Morita A, Maeda A, Hearing VJ. Regulation of skin pigmentation and thickness by Dickkopf 1 (DKK1). J Investig Dermatol Symp Proc. 2009;14(1):73-5.
42. Duve S, Schmoeckel C, Burgdorf WH. Melanocytic hyperplasia in scars. A histopathological investigation of 722 cases. Am J Dermatopathol. 1996;18(3):236-40.
43. Ferringer T. Update on immunohistochemistry in melanocytic lesions. Dermatol Clin. 2012;30(4):567-79, v.

44. Kath R, Rodeck U, Menssen HD, Mancianti ML, Linnenbach AJ, Elder DE, et al. Tumor progression in the human melanocytic system. Anticancer Res. 1989;9(4):865-72.
45. Chalmers ZR, Connelly CF, Fabrizio D, Gay L, Ali SM, Ennis R, et al. Analysis of 100,000 human cancer genomes reveals the landscape of tumor mutational burden. Genome Med. 2017;9(1):34.
46. Martincorena I, Roshan A, Gerstung M, Ellis P, Van Loo P, McLaren S, et al. Tumor evolution. High burden and pervasive positive selection of somatic mutations in normal human skin. Science. 2015;348(6237):880-6.
47. World Health Organization. Radiation: Ultraviolet (UV) radiation 2022 [Available from: https://www.who.int/news-room/questions-and-answers/item/radiation-ultraviolet-(uv).
48. Lee JW, Ratnakumar K, Hung KF, Rokunohe D, Kawasumi M. Deciphering UV-induced DNA Damage Responses to Prevent and Treat Skin Cancer. Photochem Photobiol. 2020;96(3):478-99.
49. Pissa M, Helkkula T, Appelqvist F, Silander G, Borg A, Pettersson J, et al. CDKN2A genetic testing in melanoma-prone families in Sweden in the years 2015-2020: implications for novel national recommendations. Acta Oncol. 2021;60(7):888-96.
50. Puntervoll HE, Yang XR, Vetti HH, Bachmann IM, Avril MF, Benfodda M, et al. Melanoma prone families with CDK4 germline mutation: phenotypic profile and associations with MC1R variants. J Med Genet. 2013;50(4):264-70.
51. Wiesner T, Fried I, Ulz P, Stacher E, Popper H, Murali R, et al. Toward an improved definition of the tumor spectrum associated with BAP1 germline mutations. J Clin Oncol. 2012;30(32):e337-40.
52. Wiesner T, Obenauf AC, Murali R, Fried I, Griewank KG, Ulz P, et al. Germline mutations in BAP1 predispose to melanocytic tumors. Nat Genet. 2011;43(10):1018-21.
53. Robles-Espinoza CD, Harland M, Ramsay AJ, Aoude LG, Quesada V, Ding Z, et al. POT1 loss-of-function variants predispose to familial melanoma. Nat Genet. 2014;46(5):478-81.
54. Harland M, Petljak M, Robles-Espinoza CD, Ding Z, Gruis NA, van Doorn R, et al. Germline TERT promoter mutations are rare in familial melanoma. Fam Cancer. 2016;15(1):139-44.
55. Bellenghi M, Puglisi R, Pontecorvi G, De Feo A, Care A, Mattia G. Sex and Gender Disparities in Melanoma. Cancers (Basel). 2020;12(7).
56. Landi MT, Bauer J, Pfeiffer RM, Elder DE, Hulley B, Minghetti P, et al. MC1R germline variants confer risk for BRAF-mutant melanoma. Science. 2006;313(5786):521-2.
57. Elder DE, Bastian BC, Cree IA, Massi D, Scolyer RA. The 2018 World Health Organization Classification of Cutaneous, Mucosal, and Uveal Melanoma: Detailed Analysis of 9 Distinct Subtypes Defined by Their Evolutionary Pathway. Arch Pathol Lab Med. 2020;144(4):500-22.

58. Yeh I. Update on classification of melanocytic tumors and the role of immunohistochemistry and molecular techniques. Semin Diagn Pathol. 2022;39(4):248-56.
59. Shain AH, Yeh I, Kovalyshyn I, Sriharan A, Talevich E, Gagnon A, et al. The Genetic Evolution of Melanoma from Precursor Lesions. N Engl J Med. 2015;373(20):1926-36.
60. Lee S, Barnhill RL, Dummer R, Dalton J, Wu J, Pappo A, et al. TERT Promoter Mutations Are Predictive of Aggressive Clinical Behavior in Patients with Spitzoid Melanocytic Neoplasms. Sci Rep. 2015;5:11200.
61. Mar VJ, Wong SQ, Li J, Scolyer RA, McLean C, Papenfuss AT, et al. BRAF/NRAS wild-type melanomas have a high mutation load correlating with histologic and molecular signatures of UV damage. Clin Cancer Res. 2013;19(17):4589-98.
62. Sanna A, Harbst K, Johansson I, Christensen G, Lauss M, Mitra S, et al. Tumor genetic heterogeneity analysis of chronic sun-damaged melanoma. Pigment Cell Melanoma Res. 2020;33(3):480-9.
63. Chen LL, Jaimes N, Barker CA, Busam KJ, Marghoob AA. Desmoplastic melanoma: a review. J Am Acad Dermatol. 2013;68(5):825-33.
64. Shain AH, Garrido M, Botton T, Talevich E, Yeh I, Sanborn JZ, et al. Exome sequencing of desmoplastic melanoma identifies recurrent NFKBIE promoter mutations and diverse activating mutations in the MAPK pathway. Nat Genet. 2015;47(10):1194-9.
65. Bastian BC. The molecular pathology of melanoma: an integrated taxonomy of melanocytic neoplasia. Annu Rev Pathol. 2014;9:239-71.
66. Turner J, Couts K, Sheren J, Saichaemchan S, Ariyawutyakorn W, Avolio I, et al. Kinase gene fusions in defined subsets of melanoma. Pigment Cell Melanoma Res. 2017;30(1):53-62.
67. Yeh I, Jorgenson E, Shen L, Xu M, North JP, Shain AH, et al. Targeted Genomic Profiling of Acral Melanoma. J Natl Cancer Inst. 2019;111(10):1068-77.
68. Jung HJ, Kweon SS, Lee JB, Lee SC, Yun SJ. A clinicopathologic analysis of 177 acral melanomas in Koreans: relevance of spreading pattern and physical stress. JAMA Dermatol. 2013;149(11):1281-8.
69. Hahn HM, Lee KG, Choi W, Cheong SH, Myung KB, Hahn HJ. An updated review of mucosal melanoma: Survival meta-analysis. Mol Clin Oncol. 2019;11(2):116-26.
70. Kinsler VA, O'Hare P, Bulstrode N, Calonje JE, Chong WK, Hargrave D, et al. Melanoma in congenital melanocytic naevi. Br J Dermatol. 2017;176(5):1131-43.
71. Fan Y, Lee S, Wu G, Easton J, Yergeau D, Dummer R, et al. Telomerase Expression by Aberrant Methylation of the TERT Promoter in Melanoma Arising in Giant Congenital Nevi. J Invest Dermatol. 2016;136(1):339-42.

72. Fallico M, Raciti G, Longo A, Reibaldi M, Bonfiglio V, Russo A, et al. Current molecular and clinical insights into uveal melanoma (Review). Int J Oncol. 2021;58(4).
73. National Cancer Insitute. Melanoma of the Skin,

Recent Trends in SEER Relative Survival Rates, 2004-2018 2022 [Available from: https://seer.cancer.gov/statistics-network.
74. Amin MB et al. AJCC Cancer Staging Manual, . Eight ed. New York: Springer International Publishing; 2017.
75. Garutti M, Bonin S, Buriolla S, Bertoli E, Pizzichetta MA, Zalaudek I, et al. Find the Flame: Predictive Biomarkers for Immunotherapy in Melanoma. Cancers (Basel). 2021;13(8).
76. Breslow A. Thickness, cross-sectional areas and depth of invasion in the prognosis of cutaneous melanoma. Ann Surg. 1970;172(5):902-8.
77. Rashed H, Flatman K, Bamford M, Teo KW, Saldanha G. Breslow density is a novel prognostic feature in cutaneous malignant melanoma. Histopathology. 2017;70(2):264-72.
78. Niebling MG, Haydu LE, Karim RZ, Thompson JF, Scolyer RA. Reproducibility of AJCC staging parameters in primary cutaneous melanoma: an analysis of 4,924 cases. Ann Surg Oncol. 2013;20(12):3969-75.
79. Thompson JF, Soong SJ, Balch CM, Gershenwald JE, Ding S, Coit DG, et al. Prognostic significance of mitotic rate in localized primary cutaneous melanoma: an analysis of patients in the multi-institutional American Joint Committee on Cancer melanoma staging database. J Clin Oncol. 2011;29(16):2199-205.
80. Balch CM, Gershenwald JE, Soong SJ, Thompson JF, Atkins MB, Byrd DR, et al. Final version of 2009 AJCC melanoma staging and classification. J Clin Oncol. 2009;27(36):6199-206.
81. Gershenwald JE, Scolyer RA. Melanoma Staging: American Joint Committee on Cancer (AJCC) 8th Edition and Beyond. Ann Surg Oncol. 2018;25(8):2105-10.
82. Saldanha G, Ali R, Bakshi A, Basiouni A, Bishop R, Colloby P, et al. Global and mitosis-specific interobserver variation in mitotic count scoring and implications for malignant melanoma staging. Histopathology. 2020;76(6):803-13.
83. Wang M, Aung PP, Prieto VG. Standardized Method for Defining a 1-mm2 Region of Interest for Calculation of Mitotic Rate on Melanoma Whole Slide Images. Arch Pathol Lab Med. 2021;145(10):1255-63.
84. Cochran AJ, Wen DR, Morton DL. Management of the regional lymph nodes in patients with cutaneous malignant melanoma. World J Surg. 1992;16(2):214-21.

85. Morton DL, Wen DR, Wong JH, Economou JS, Cagle LA, Storm FK, et al. Technical details of intraoperative lymphatic mapping for early stage melanoma. Arch Surg. 1992;127(4):392-9.
86. Morton DL, Cochran AJ, Thompson JF, Elashoff R, Essner R, Glass EC, et al. Sentinel node biopsy for early-stage melanoma: accuracy and morbidity in MSLT-I, an international multicenter trial. Ann Surg. 2005;242(3):302-11; discussion 11-3.
87. Mirzaei N, Katsarelias D, Zaar P, Jalnefjord O, Johansson I, Leonhardt H, et al. Sentinel lymph node localization and staging with a low-dose of superparamagnetic iron oxide (SPIO) enhanced MRI and magnetometer in patients with cutaneous melanoma of the extremity - The MAGMEN feasibility study. Eur J Surg Oncol. 2022;48(2):326-32.
88. Lobo AZ, Tanabe KK, Luo S, Muzikansky A, Sober AJ, Tsao H, et al. The distribution of microscopic melanoma metastases in sentinel lymph nodes: implications for pathology protocols. Am J Surg Pathol. 2012;36(12):1841-8.
89. Huang H, Fu Z, Ji J, Huang J, Long X. Predictive Values of Pathological and Clinical Risk Factors for Positivity of Sentinel Lymph Node Biopsy in Thin Melanoma: A Systematic Review and Meta-Analysis. Front Oncol. 2022;12:817510.
90. Isaksson K, Nielsen K, Mikiver R, Nieweg OE, Scolyer RA, Thompson JF, et al. Sentinel lymph node biopsy in patients with thin melanomas: Frequency and predictors of metastasis based on analysis of two large international cohorts. J Surg Oncol. 2018;118(4):599-605.
91. Han D, Han G, Duque MT, Morrison S, Leong SP, Kashani-Sabet M, et al. Sentinel Lymph Node Biopsy Is Prognostic in Thickest Melanoma Cases and Should Be Performed for Thick Melanomas. Ann Surg Oncol. 2021;28(2):1007-16.
92. Moncrieff MD, Lo SN, Scolyer RA, Heaton MJ, Nobes JP, Snelling AP, et al. Clinical Outcomes and Risk Stratification of Early-Stage Melanoma Micrometastases From an International Multicenter Study: Implications for the Management of American Joint Committee on Cancer IIIA Disease. J Clin Oncol. 2022:JCO2102488.
93. Socialstyrelsen. Nationellt vårdprogram för malignt melanom. Prognosinstrument för melanom 2022 [Available from: https://kunskapsbanken.cancercentrum.se/diagnoser/melanom/vardprogram/prognosinstrument.
94. Memorial Sloan Kettering Cancer Center. Melanoma nomogram 2022 [Available from: https://www.mskcc.org/nomograms/melanoma/sentinel_lymph_node_metastasis.
95. Pasquali S, Mocellin S, Campana LG, Vecchiato A, Bonandini E, Montesco MC, et al. Maximizing the clinical usefulness of a nomogram to select patients candidate to sentinel node biopsy for cutaneous melanoma. Eur J Surg Oncol. 2011;37(8):675-80.

96. Melanoma Institute Australia. Risk Prediction Tools, Sentinel Node Metastasis Risk 2022 [Available from: https://www.melanomarisk.org.au/SNLForm.
97. Lo SN, Ma J, Scolyer RA, Haydu LE, Stretch JR, Saw RPM, et al. Improved Risk Prediction Calculator for Sentinel Node Positivity in Patients With Melanoma: The Melanoma Institute Australia Nomogram. J Clin Oncol. 2020;38(24):2719-27.
98. El Sharouni MA, Varey AHR, Witkamp AJ, Ahmed T, Sigurdsson V, van Diest PJ, et al. Predicting sentinel node positivity in patients with melanoma: external validation of a risk-prediction calculator (the Melanoma Institute Australia nomogram) using a large European population-based patient cohort. Br J Dermatol. 2021;185(2):412-8.
99. Melanoma Institute Australia. Risk Prediction Tools, Thin Melaoma Recurrence Risk [Available from: https://www.melanomarisk.org.au/ThinMelForm.
100. El Sharouni MA, Ahmed T, Varey AHR, Elias SG, Witkamp AJ, Sigurdsson V, et al. Development and Validation of Nomograms to Predict Local, Regional, and Distant Recurrence in Patients With Thin (T1) Melanomas. J Clin Oncol. 2021;39(11):1243-52.
101. Bai X, Kong Y, Chi Z, Sheng X, Cui C, Wang X, et al. MAPK Pathway and TERT Promoter Gene Mutation Pattern and Its Prognostic Value in Melanoma Patients: A Retrospective Study of 2,793 Cases. Clin Cancer Res. 2017;23(20):6120-7.
102. Clarke LE, Flake DD, 2nd, Busam K, Cockerell C, Helm K, McNiff J, et al. An independent validation of a gene expression signature to differentiate malignant melanoma from benign melanocytic nevi. Cancer. 2017;123(4):617-28.
103. Gerami P, Cook RW, Wilkinson J, Russell MC, Dhillon N, Amaria RN, et al. Development of a prognostic genetic signature to predict the metastatic risk associated with cutaneous melanoma. Clin Cancer Res. 2015;21(1):175-83.
104. Brunner G, Reitz M, Heinecke A, Lippold A, Berking C, Suter L, et al. A nine-gene signature predicting clinical outcome in cutaneous melanoma. J Cancer Res Clin Oncol. 2013;139(2):249-58.
105. Bellomo D, Arias-Mejias SM, Ramana C, Heim JB, Quattrocchi E, Sominidi-Damodaran S, et al. Model Combining Tumor Molecular and Clinicopathologic Risk Factors Predicts Sentinel Lymph Node Metastasis in Primary Cutaneous Melanoma. JCO Precis Oncol. 2020;4:319-34.
106. Johansson I, Tempel D, Dwarkasing JT, Rentroia-Pacheco B, Mattsson J, Ny L, et al. Validation of a clinicopathological and gene expression profile model to identify patients with cutaneous melanoma where sentinel lymph node biopsy is unnecessary. Eur J Surg Oncol. 2022;48(2):320-5.
107. Chapman BC, Goodman K, Hosokawa P, Gleisner A, Cowan ML, Birnbaum E, et al. Improved survival in rectal cancer patients who are

treated with long-course versus short-course neoadjuvant radiotherapy: A propensity-matched analysis of the NCDB. J Surg Oncol. 2019;119(4):518-31.
108. Pham DDM, Guhan S, Tsao H. KIT and Melanoma: Biological Insights and Clinical Implications. Yonsei Med J. 2020;61(7):562-71.
109. Sha D, Jin Z, Budczies J, Kluck K, Stenzinger A, Sinicrope FA. Tumor Mutational Burden as a Predictive Biomarker in Solid Tumors. Cancer Discov. 2020;10(12):1808-25.
110. Madore J, Vilain RE, Menzies AM, Kakavand H, Wilmott JS, Hyman J, et al. PD-L1 expression in melanoma shows marked heterogeneity within and between patients: implications for anti-PD-1/PD-L1 clinical trials. Pigment Cell Melanoma Res. 2015;28(3):245-53.
111. Vilain RE, Menzies AM, Wilmott JS, Kakavand H, Madore J, Guminski A, et al. Dynamic Changes in PD-L1 Expression and Immune Infiltrates Early During Treatment Predict Response to PD-1 Blockade in Melanoma. Clin Cancer Res. 2017;23(17):5024-33.
112. Diggs LP, Hsueh EC. Utility of PD-L1 immunohistochemistry assays for predicting PD-1/PD-L1 inhibitor response. Biomark Res. 2017;5:12.
113. Torlakovic E, Lim HJ, Adam J, Barnes P, Bigras G, Chan AWH, et al. "Interchangeability" of PD-L1 immunohistochemistry assays: a meta-analysis of diagnostic accuracy. Mod Pathol. 2020;33(1):4-17.
114. Kempf W, Mertz KD, Hofbauer GF, Tinguely M. Skin cancer in organ transplant recipients. Pathobiology. 2013;80(6):302-9.
115. Cabrita R, Lauss M, Sanna A, Donia M, Skaarup Larsen M, Mitra S, et al. Tertiary lymphoid structures improve immunotherapy and survival in melanoma. Nature. 2020;577(7791):561-5.
116. Ovcinnikovs V, Ross EM, Petersone L, Edner NM, Heuts F, Ntavli E, et al. CTLA-4-mediated transendocytosis of costimulatory molecules primarily targets migratory dendritic cells. Sci Immunol. 2019;4(35).
117. Bruno TC, Ebner PJ, Moore BL, Squalls OG, Waugh KA, Eruslanov EB, et al. Antigen-Presenting Intratumoral B Cells Affect CD4(+) TIL Phenotypes in Non-Small Cell Lung Cancer Patients. Cancer Immunol Res. 2017;5(10):898-907.
118. Germain C, Gnjatic S, Tamzalit F, Knockaert S, Remark R, Goc J, et al. Presence of B cells in tertiary lymphoid structures is associated with a protective immunity in patients with lung cancer. Am J Respir Crit Care Med. 2014;189(7):832-44.
119. Zhou L, Xu B, Liu Y, Wang Z. Tertiary lymphoid structure signatures are associated with survival and immunotherapy response in muscle-invasive bladder cancer. Oncoimmunology. 2021;10(1):1915574.
120. Sautes-Fridman C, Petitprez F, Calderaro J, Fridman WH. Tertiary lymphoid structures in the era of cancer immunotherapy. Nat Rev Cancer. 2019;19(6):307-25.
121. Lauss M, Donia M, Svane IM, Jonsson G. B Cells and Tertiary Lymphoid Structures: Friends or Foes in Cancer Immunotherapy? Clin Cancer Res. 2022;28(9):1751-8.

122. Regionala Cancercenrum i samverkan. Nationellt vårdprogram melanom 2022 [Available from: https://kunskapsbanken.cancercentrum.se/diagnoser/melanom/vardprogram/.
123. Leung AM, Morton DL, Ozao-Choy J, Hari DM, Shin-Sim M, Difronzo AL, et al. Staging of regional lymph nodes in melanoma: a case for including nonsentinel lymph node positivity in the American Joint Committee on Cancer staging system. JAMA Surg. 2013;148(9):879-84.
124. Leiter U, Stadler R, Mauch C, Hohenberger W, Brockmeyer N, Berking C, et al. Complete lymph node dissection versus no dissection in patients with sentinel lymph node biopsy positive melanoma (DeCOG-SLT): a multicentre, randomised, phase 3 trial. Lancet Oncol. 2016;17(6):757-67.
125. Faries MB, Thompson JF, Cochran AJ, Andtbacka RH, Mozzillo N, Zager JS, et al. Completion Dissection or Observation for Sentinel-Node Metastasis in Melanoma. N Engl J Med. 2017;376(23):2211-22.
126. Cancer Genome Atlas N. Genomic Classification of Cutaneous Melanoma. Cell. 2015;161(7):1681-96.
127. Nebhan CA, Johnson DB, Sullivan RJ, Amaria RN, Flaherty KT, Sosman JA, et al. Efficacy and Safety of Trametinib in Non-V600 BRAF Mutant Melanoma: A Phase II Study. Oncologist. 2021;26(9):731-e1498.
128. Delyon J, Lebbe C, Dumaz N. Targeted therapies in melanoma beyond BRAF: targeting NRAS-mutated and KIT-mutated melanoma. Curr Opin Oncol. 2020;32(2):79-84.
129. Hodi FS, Corless CL, Giobbie-Hurder A, Fletcher JA, Zhu M, Marino-Enriquez A, et al. Imatinib for melanomas harboring mutationally activated or amplified KIT arising on mucosal, acral, and chronically sun-damaged skin. J Clin Oncol. 2013;31(26):3182-90.
130. Long GV, Margolin KA. Multidisciplinary approach to brain metastasis from melanoma: the emerging role of systemic therapies. Am Soc Clin Oncol Educ Book. 2013:393-8.
131. Budman DR, Camacho E, Wittes RE. The current causes of death in patients with malignant melanoma. Eur J Cancer (1965). 1978;14(4):327-30.
132. Vosoughi E, Lee JM, Miller JR, Nosrati M, Minor DR, Abendroth R, et al. Survival and clinical outcomes of patients with melanoma brain metastasis in the era of checkpoint inhibitors and targeted therapies. BMC Cancer. 2018;18(1):490.
133. Patel JK, Didolkar MS, Pickren JW, Moore RH. Metastatic pattern of malignant melanoma. A study of 216 autopsy cases. Am J Surg. 1978;135(6):807-10.
134. Fife KM, Colman MH, Stevens GN, Firth IC, Moon D, Shannon KF, et al. Determinants of outcome in melanoma patients with cerebral metastases. J Clin Oncol. 2004;22(7):1293-300.

135. Cheli Y, Bonnazi VF, Jacquel A, Allegra M, De Donatis GM, Bahadoran P, et al. CD271 is an imperfect marker for melanoma initiating cells. Oncotarget. 2014;5(14):5272-83.
136. Choi SS, Lee HJ, Lim I, Satoh J, Kim SU. Human astrocytes: secretome profiles of cytokines and chemokines. PLoS One. 2014;9(4):e92325.
137. Gardner LJ, Ward M, Andtbacka RHI, Boucher KM, Bowen GM, Bowles TL, et al. Risk factors for development of melanoma brain metastasis and disease progression: a single-center retrospective analysis. Melanoma Res. 2017;27(5):477-84.
138. Argenziano G, Catricala C, Ardigo M, Buccini P, De Simone P, Eibenschutz L, et al. Seven-point checklist of dermoscopy revisited. Br J Dermatol. 2011;164(4):785-90.
139. Argenziano G, Fabbrocini G, Carli P, De Giorgi V, Sammarco E, Delfino M. Epiluminescence microscopy for the diagnosis of doubtful melanocytic skin lesions. Comparison of the ABCD rule of dermatoscopy and a new 7-point checklist based on pattern analysis. Arch Dermatol. 1998;134(12):1563-70.
140. Petersen BS, Fredrich B, Hoeppner MP, Ellinghaus D, Franke A. Opportunities and challenges of whole-genome and -exome sequencing. BMC Genet. 2017;18(1):14.
141. Kukurba KR, Montgomery SB. RNA Sequencing and Analysis. Cold Spring Harb Protoc. 2015;2015(11):951-69.
142. Mulder E, Dwarkasing JT, Tempel D, van der Spek A, Bosman L, Verver D, et al. Validation of a clinicopathological and gene expression profile model for sentinel lymph node metastasis in primary cutaneous melanoma. Br J Dermatol. 2021;184(5):944-51.
143. National Comprehensive Cancer Network. NCCN Guidelines Version 3.2022

Melanoma: Cutaneous 2022 [Available from: https://www.nccn.org/professionals/physician_gls/pdf/cutaneous_melanoma.pdf.
144. Verver D, van Klaveren D, Franke V, van Akkooi ACJ, Rutkowski P, Keilholz U, et al. Development and validation of a nomogram to predict recurrence and melanoma-specific mortality in patients with negative sentinel lymph nodes. Br J Surg. 2019;106(3):217-25.
145. El Sharouni MA, Ahmed T, Witkamp AJ, Sigurdsson V, van Gils CH, Nieweg OE, et al. Predicting recurrence in patients with sentinel node-negative melanoma: validation of the EORTC nomogram using population-based data. Br J Surg. 2021;108(5):550-3.
146. Menzies AM, Haydu LE, Visintin L, Carlino MS, Howle JR, Thompson JF, et al. Distinguishing clinicopathologic features of patients with V600E and V600K BRAF-mutant metastatic melanoma. Clin Cancer Res. 2012;18(12):3242-9.

147. Stadelmeyer E, Heitzer E, Resel M, Cerroni L, Wolf P, Dandachi N. The BRAF V600K mutation is more frequent than the BRAF V600E mutation in melanoma in situ of lentigo maligna type. J Invest Dermatol. 2014;134(2):548-50.
148. Smoller BR. Histologic criteria for diagnosing primary cutaneous malignant melanoma. Mod Pathol. 2006;19 Suppl 2:S34-40.
149. Rastogi RP, Richa, Kumar A, Tyagi MB, Sinha RP. Molecular mechanisms of ultraviolet radiation-induced DNA damage and repair. J Nucleic Acids. 2010;2010:592980.
150. Alexandrov LB, Nik-Zainal S, Wedge DC, Aparicio SA, Behjati S, Biankin AV, et al. Signatures of mutational processes in human cancer. Nature. 2013;500(7463):415-21.
151. Evidencio MDS. Nomogram predicting recurrence and melanoma-specific mortality in patients with negative sentinel lymph nodes 2022 [Available from: https://www.evidencio.com/models/show/1890.
152. Berger MF, Hodis E, Heffernan TP, Deribe YL, Lawrence MS, Protopopov A, et al. Melanoma genome sequencing reveals frequent PREX2 mutations. Nature. 2012;485(7399):502-6.
153. Cirenajwis H, Lauss M, Ekedahl H, Torngren T, Kvist A, Saal LH, et al. NF1-mutated melanoma tumors harbor distinct clinical and biological characteristics. Mol Oncol. 2017;11(4):438-51.
154. Hayward NK, Wilmott JS, Waddell N, Johansson PA, Field MA, Nones K, et al. Whole-genome landscapes of major melanoma subtypes. Nature. 2017;545(7653):175-80.
155. Hodis E, Watson IR, Kryukov GV, Arold ST, Imielinski M, Theurillat JP, et al. A landscape of driver mutations in melanoma. Cell. 2012;150(2):251-63.
156. Krauthammer M, Kong Y, Ha BH, Evans P, Bacchiocchi A, McCusker JP, et al. Exome sequencing identifies recurrent somatic RAC1 mutations in melanoma. Nat Genet. 2012;44(9):1006-14.
157. Eroglu Z, Zaretsky JM, Hu-Lieskovan S, Kim DW, Algazi A, Johnson DB, et al. High response rate to PD-1 blockade in desmoplastic melanomas. Nature. 2018;553(7688):347-50.
158. Shain AH, Bastian BC. The Genetic Evolution of Melanoma. N Engl J Med. 2016;374(10):995-6.
159. Mattsson J, Bergkvist L, Abdiu A, Aili Low JF, Naredi P, Ullberg K, et al. Sentinel node biopsy in malignant melanoma: Swedish experiences 1997-2005. Acta Oncol. 2008;47(8):1519-25.
160. Gjorup CA, Groenvold M, Hendel HW, Dahlstroem K, Drzewiecki KT, Klausen TW, et al. Health-related quality of life in melanoma patients: Impact of melanoma-related limb lymphoedema. Eur J Cancer. 2017;85:122-32.
161. Kretschmer L, Thoms KM, Peeters S, Haenssle H, Bertsch HP, Emmert S. Postoperative morbidity of lymph node excision for cutaneous

melanoma-sentinel lymphonodectomy versus complete regional lymph node dissection. Melanoma Res. 2008;18(1):16-21.
162. Dummer R, Hauschild A, Santinami M, Atkinson V, Mandala M, Kirkwood JM, et al. Five-Year Analysis of Adjuvant Dabrafenib plus Trametinib in Stage III Melanoma. N Engl J Med. 2020;383(12):1139-48.
163. Eggermont AMM, Blank CU, Mandala M, Long GV, Atkinson VG, Dalle S, et al. Longer Follow-Up Confirms Recurrence-Free Survival Benefit of Adjuvant Pembrolizumab in High-Risk Stage III Melanoma: Updated Results From the EORTC 1325-MG/KEYNOTE-054 Trial. J Clin Oncol. 2020;38(33):3925-36.
164. Ascierto PA, Del Vecchio M, Mandala M, Gogas H, Arance AM, Dalle S, et al. Adjuvant nivolumab versus ipilimumab in resected stage IIIB-C and stage IV melanoma (CheckMate 238): 4-year results from a multicentre, double-blind, randomised, controlled, phase 3 trial. Lancet Oncol. 2020;21(11):1465-77.
165. Whiteman DC, Baade PD, Olsen CM. More people die from thin melanomas (1 mm) than from thick melanomas (>4 mm) in Queensland, Australia. J Invest Dermatol. 2015;135(4):1190-3.
166. Landow SM, Gjelsvik A, Weinstock MA. Mortality burden and prognosis of thin melanomas overall and by subcategory of thickness, SEER registry data, 1992-2013. J Am Acad Dermatol. 2017;76(2):258-63.
167. Gershenwald JE, Scolyer RA, Hess KR, Sondak VK, Long GV, Ross MI, et al. Melanoma staging: Evidence-based changes in the American Joint Committee on Cancer eighth edition cancer staging manual. CA Cancer J Clin. 2017;67(6):472-92.
168. Lyth J, Mikiver R, Nielsen K, Isaksson K, Ingvar C. Prognostic instrument for survival outcome in melanoma patients: based on data from the population-based Swedish Melanoma Register. Eur J Cancer. 2016;59:171-8.
169. Thakur R, Laye JP, Lauss M, Diaz JMS, O'Shea SJ, Pozniak J, et al. Transcriptomic Analysis Reveals Prognostic Molecular Signatures of Stage I Melanoma. Clin Cancer Res. 2019;25(24):7424-35.
170. Zager JS, Gastman BR, Leachman S, Gonzalez RC, Fleming MD, Ferris LK, et al. Performance of a prognostic 31-gene expression profile in an independent cohort of 523 cutaneous melanoma patients. BMC Cancer. 2018;18(1):130.
171. Cook RW, Middlebrook B, Wilkinson J, Covington KR, Oelschlager K, Monzon FA, et al. Analytic validity of DecisionDx-Melanoma, a gene expression profile test for determining metastatic risk in melanoma patients. Diagn Pathol. 2018;13(1):13.
172. Hsueh EC, DeBloom JR, Lee JH, Sussman JJ, Covington KR, Caruso HG, et al. Long-Term Outcomes in a Multicenter, Prospective Cohort Evaluating the Prognostic 31-Gene Expression Profile for Cutaneous Melanoma. JCO Precis Oncol. 2021;5.
173. Gastman BR, Gerami P, Kurley SJ, Cook RW, Leachman S, Vetto JT. Identification of patients at risk of metastasis using a prognostic 31-

gene expression profile in subpopulations of melanoma patients with favorable outcomes by standard criteria. J Am Acad Dermatol. 2019;80(1):149-57 e4.
174. Marchetti MA, Bartlett EK, Dusza SW, Bichakjian CK. Use of a prognostic gene expression profile test for T1 cutaneous melanoma: Will it help or harm patients? J Am Acad Dermatol. 2019;80(6):e161-e2.
175. Amaral TMS, Hoffmann MC, Sinnberg T, Niessner H, Sulberg H, Eigentler TK, et al. Clinical validation of a prognostic 11-gene expression profiling score in prospectively collected FFPE tissue of patients with AJCC v8 stage II cutaneous melanoma. Eur J Cancer. 2020;125:38-45.
176. Marchetti MA, Coit DG, Dusza SW, Yu A, McLean L, Hu Y, et al. Performance of Gene Expression Profile Tests for Prognosis in Patients With Localized Cutaneous Melanoma: A Systematic Review and Meta-analysis. JAMA Dermatol. 2020;156(9):953-62.
177. Garg M, Couturier DL, Nsengimana J, Fonseca NA, Wongchenko M, Yan Y, et al. Tumour gene expression signature in primary melanoma predicts long-term outcomes. Nat Commun. 2021;12(1):1137.
178. Luke JJ, Rutkowski P, Queirolo P, Del Vecchio M, Mackiewicz J, Chiarion-Sileni V, et al. Pembrolizumab versus placebo as adjuvant therapy in completely resected stage IIB or IIC melanoma (KEYNOTE-716): a randomised, double-blind, phase 3 trial. Lancet. 2022;399(10336):1718-29.
179. Kovarik CL, Chu EY, Adamson AS. Gene Expression Profile Testing for Thin Melanoma: Evidence to Support Clinical Use Remains Thin. JAMA Dermatol. 2020;156(8):837-8.
180. Clark WH, Jr., From L, Bernardino EA, Mihm MC. The histogenesis and biologic behavior of primary human malignant melanomas of the skin. Cancer Res. 1969;29(3):705-27.
181. Clark WH, Jr., Elder DE, Guerry Dt, Braitman LE, Trock BJ, Schultz D, et al. Model predicting survival in stage I melanoma based on tumor progression. J Natl Cancer Inst. 1989;81(24):1893-904.
182. Clemente CG, Mihm MC, Jr., Bufalino R, Zurrida S, Collini P, Cascinelli N. Prognostic value of tumor infiltrating lymphocytes in the vertical growth phase of primary cutaneous melanoma. Cancer. 1996;77(7):1303-10.
183. Lee N, Zakka LR, Mihm MC, Jr., Schatton T. Tumour-infiltrating lymphocytes in melanoma prognosis and cancer immunotherapy. Pathology. 2016;48(2):177-87.
184. Chen DS, Mellman I. Oncology meets immunology: the cancer-immunity cycle. Immunity. 2013;39(1):1-10.
185. Saldanha G, Flatman K, Teo KW, Bamford M. A Novel Numerical Scoring System for Melanoma Tumor-infiltrating Lymphocytes Has Better Prognostic Value Than Standard Scoring. Am J Surg Pathol. 2017;41(7):906-14.
186. Griss J, Bauer W, Wagner C, Simon M, Chen M, Grabmeier-Pfistershammer K, et al. B cells sustain inflammation and predict response to immune checkpoint blockade in human melanoma. Nat Commun. 2019;10(1):4186.